iScience

CellPress
OPEN ACCESS

Article

Regulation of hierarchical carbon substrate utilization, nitrogen fixation, and root colonization by the Hfq/Crc/CrcZY genes in *Pseudomonas stutzeri*

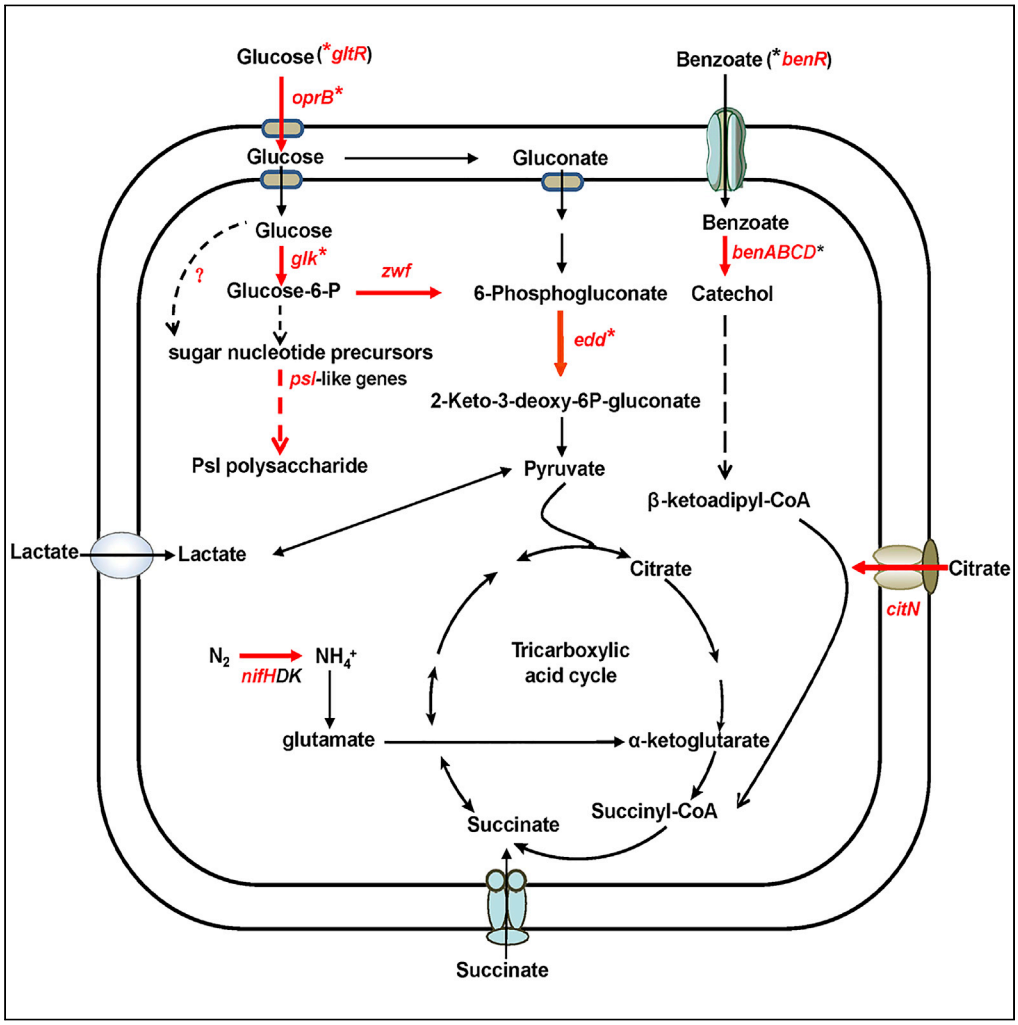

Fanyang Lv, Yuhua Zhan, Wei Lu, ..., Claudine Elmerich, Yongliang Yan, Min Lin

yanyongliang@caas.cn (Y.Y.)
linmin@caas.cn (M.L.)

Highlights

A1501 preferentially catabolizes succinate followed by citrate and ultimately glucose

The Hfq/Crc/CrcZY regulatory system orchestrates this preference

Hfq optimizes nitrogen fixation and root colonization

Glucose is shunted into an unidentified route to produce Psl exopolysaccharide

Lv et al., iScience 25, 105663
December 22, 2022 © 2022
https://doi.org/10.1016/j.isci.2022.105663

iScience

CellPress
OPEN ACCESS

Article

Regulation of hierarchical carbon substrate utilization, nitrogen fixation, and root colonization by the Hfq/Crc/CrcZY genes in *Pseudomonas stutzeri*

Fanyang Lv,[1,4] Yuhua Zhan,[1,4] Wei Lu,[1] Xiubin Ke,[1] Yahui Shao,[1] Yiyuan Ma,[1] Juan Zheng,[1] Zhimin Yang,[1] Shanshan Jiang,[1] Liguo Shang,[1] Yao Ma,[1] Lei Cheng,[2] Claudine Elmerich,[3] Yongliang Yan,[1,*] and Min Lin[1,2,5,*]

SUMMARY

Bacteria of the genus *Pseudomonas* consume preferred carbon substrates in nearly reverse order to that of enterobacteria, and this process is controlled by RNA-binding translational repressors and regulatory ncRNA antagonists. However, their roles in microbe-plant interactions and the underlying mechanisms remain uncertain. Here we show that root-associated diazotrophic *Pseudomonas stutzeri* A1501 preferentially catabolizes succinate, followed by the less favorable substrate citrate, and ultimately glucose. Furthermore, the Hfq/Crc/CrcZY regulatory system orchestrates this preference and contributes to optimal nitrogenase activity and efficient root colonization. Hfq has a central role in this regulatory network through different mechanisms of action, including repressing the translation of substrate-specific catabolic genes, activating the nitrogenase gene *nifH* posttranscriptionally, and exerting a positive effect on the transcription of an exopolysaccharide gene cluster. Our results illustrate an Hfq-mediated mechanism linking carbon metabolism to nitrogen fixation and root colonization, which may confer rhizobacteria competitive advantages in rhizosphere environments.

INTRODUCTION

Bacteria can utilize numerous carbon substrates, and thus they can grow in a wide range of natural environments. Carbon substrates in the environment variable in type and abundance and can be utilized by bacteria either hierarchically or simultaneously.[1] Hierarchical utilization refers to catabolite repression, in which preferred carbon sources prevent the utilization of other substrates, and a variety of mechanisms are used, depending on the bacterial genus[2,3]; the classic example of which is glucose-lactose diauxic growth of *Escherichia coli*.[4] It is now well accepted that carbon catabolite repression controls the sequential catabolism of preferred carbon substrates, thereby enhancing the ability of bacteria to compete in their natural habitats.[5] Bacteria of the genus *Pseudomonas* are considered generalists because they are isolated from a wide range of niches and have the remarkable property of metabolizing a wide range of compounds as a source of carbon and energy.[6,7] *Pseudomonas* are metabolically versatile and behave as intelligent eaters that preferentially catabolize organic acids, especially tricarboxylic acid (TCA) cycle intermediates, rather than carbohydrates.[5,8,9] Clearly, pseudomonads use a "reverse" carbon catabolite repression compared to enterobacteria, which may reflect better adaptation to specific environments due to the differential evolution that occurs in different niches.

Indeed, the molecular mechanisms responsible for carbon catabolite repression differ markedly among microorganisms. In particular, catabolite repression is mediated at the transcription level in *E. coli* (by the Crp transcriptional regulator) and *Bacillus subtilis* (by the CcpA transcriptional regulator) while in *Pseudomonas*, carbon catabolite repression operates at the translational level.[3,5] The current model that was derived from studies of different *Pseudomonas* species showed that in this posttranscriptional repression system, the major players are the RNA chaperone Hfq, the catabolite repression control protein Crc and several regulatory ncRNAs.[10–12] In the presence of preferred carbon sources, the translation of target genes involved in the utilization of non-preferred carbon sources is inhibited by Hfq by forming a repressive complex with Crc on specific target mRNAs.[13,14] Emerging evidence further revealed that Hfq recognizes

[1]Biotechnology Research Institute/Key Laboratory of Agricultural Microbiome (MARA), Chinese Academy of Agricultural Sciences, Beijing, China

[2]Key Laboratory of Development and Application of Rural Renewable Energy, Biogas Institute of Ministry of Agriculture and Rural Affairs, Chengdu, China

[3]Institut Pasteur, Paris, France

[4]These authors contributed equally

[5]Lead contact

*Correspondence: yanyongliang@caas.cn (Y.Y.), linmin@caas.cn (M.L.)

https://doi.org/10.1016/j.isci.2022.105663

This is an open access article under the CC BY-NC-ND license (http://creativecommons.org/licenses/by-nc-nd/4.0/).

and binds to target mRNAs containing a common catabolite activity (CA) motif that is located close to the ribosome binding site[14]; in contrast, Crc has no intrinsic RNA-binding activity[15] but increases the stability of the Hfq/Crc/mRNA tripartite complexes.[10] Sequences that resemble the CA motif are present in mRNAs of the *oprB1*, *gtsABC*, *benR*, *benA*, *alkS*, and *alkB* genes in *Pseudomonas putida*,[16–19] the *amiE*, *antR*, *estA*, *bkdR* and *aroP2* genes in *Pseudomonas aeruginosa*,[20–22] the *xutR* and *xutA* genes in *Pseudomonas fluorescens*,[23] *oprB* in *Pseudomonas syringae*,[24] and *gluP* in *Azotobacter vinelandii*,[25] which are involved in the utilization of non-preferred carbon sources. Several regulatory ncRNAs, such as CrcZ in *P. aeruginosa*,[19,26] CrcZ/CrcY in *P. putida* or *P. fluorescens*,[23,27] and CrcZ/CrcX in *P. syringae*,[27] have been identified as antagonists of catabolite repression. Synthesis of these ncRNA is under the control of the two-component system CbrAB and the alternative sigma factor RpoN,[20,23,27,28] with one exception for CrcY, in which the activation is thought to involve a different transcriptional regulator in *P. putida*.[27]

Although carbon catabolite repression in bacteria is one of the best-studied metabolic strategies, we are far from understanding the complexity of this regulatory system. Mechanisms that operate in carbon catabolite repression seem to control not only the expression of the genes involved in specific catabolic pathways but also the expression of the genes involved in microbe-plant interactions.[5,29] For example, the control of catabolite repression was also found to be necessary for the growth and survival of *P. syringae* DC3000 during infection[30] and the mineral phosphate-solubilizing/glycine betaine-producing ability of *Acinetobacter* sp. SK2[31] and *P. aeruginosa*.[32,33] Similarly, the involvement of catabolite repression control in functions related to bacteria-plant interactions has been reported in *Klebsiella pneumoniae*[34] and *Rhizobium* sp.,[35] suggesting that this mechanism is widespread among rhizobacteria. In addition, the rhizosphere is a nitrogen-limiting environment that favors the proliferation of diazotrophs; the energy necessary to sustain root-associated nitrogen fixation is derived from the oxidation of carbon-rich exudates available in the rhizosphere.[36,37] Therefore, another interesting emerging aspect is the connection between carbon catabolite repression and nitrogen fixation in root-associated diazotrophs.

Bacterial species belonging to the *Pseudomonas* genus are very efficient colonizers of the plant rhizosphere, resulting from the co-occurrence of multiple functions, such as chemotactic motility, surface attachment, biofilm formation, stress response, and nitrogen fixation.[38–42] One of the most representative strains is *Pseudomonas stutzeri* A1501, a model diazotroph that was originally isolated from the rice rhizosphere.[6] Due to its nitrogen-fixing ability, A1501 outcompetes other soil bacteria and proliferates in the carbon-rich but nitrogen-limiting environment of the rhizosphere to colonize root surface or inner cortex, and benefit host plant growth.[43,44] Several genes (e.g., *cbrAB*, *crc*, and *crcZ*) involved in catabolite repression have been previously identified in *P. stutzeri* A1501.[45] A subsequent transcriptional analysis of the *P. stutzeri* A1501 genome resulted in the identification of 53 ncRNAs, including *crcZ* and *crcY*.[46] In addition, the chaperone gene Hfq was found to play a role in the control of nitrogen fixation, since an *hfq* mutant strain displayed reduced nitrogenase activity,[46,47] although the actual mechanism of this regulation remains to be documented.

In this study, we focused on performing a detailed analysis of the genetic determinants involved in catabolite repression control, as well as some of the target genes involved in this mechanism, to better understand the regulatory mechanisms underlying hierarchical carbon substrate utilization in root-associated diazotrophic *P. stutzeri* A1501. We found that *P. stutzeri* A1501 preferentially catabolized succinate, followed by the relatively less favorable substrate citrate, and ultimately glucose. Genetic studies and microscale thermophoresis (MST) experiments showed that Hfq represses the translation of catabolic targets for non-preferred substrates by binding directly to mRNAs while Crc interacts with Hfq, enhancing the repression exerted by Hfq. Subsequent physiological and droplet digital PCR (ddPCR) analysis indicated that non-preferred carbon sources such as glucose and benzoate substantially increased the transcription of CrcZ, acting as a key antagonist of Hfq, by binding the protein and relieving the repression of the non-preferred catabolic pathways. Finally, our finding provides empirical evidence for the molecular mechanism by which Hfq contributes to optimal nitrogenase activity and efficient root colonization.

RESULTS

Carbon substrate utilization profile and diauxic growth

The hierarchy of carbon substrate utilization was determined by measuring the respiratory activity and growth ability of strain A1501 grown on single or double carbon sources. We first measured the respiratory activity on different carbon sources by using Biolog GENIII MicroPlates. Forty-three compounds that

supported metabolism were identified and grouped by their intensities of respiratory activity into two distinct groups (Table S1). Interestingly, many carbon sources from the MicroPlates are also present in plant root exudates,[40] such as lactate, glucose, succinate, and citrate, with strong respiratory activities from 1694 to 1175 U (Table S1).

These data agree with the fact that organic acids are known to be preferentially used over sugars and aromatic compounds in *Pseudomonas* species. *P. stutzeri* A1501 displays better growth with lactate, succinate, or citrate than with glucose or benzoate, as shown in Figure 1A. The results from the growth assay were consistent with those of the Biolog assay (Table S1), except for glucose, supporting the high respiratory activity but poor growth of strain A1501. In addition, the carbon source preference is almost consistent with the capacity to support nitrogenase activity (Figure 1B), except for benzoate that does not support nitrogen fixation. In addition, strain A1501 preferentially utilized an organic acid until it was exhausted and then shifted to catabolism of glucose, exhibiting typical diauxic growth (Figures 1C–1E).

A1501 was previously shown to grow on 4 mM benzoate but rarely grew on 8 mM benzoate due to its toxic effect.[48] Here we observed that in the presence of 4 mM benzoate plus succinate or lactate, A1501 was able to grow well but did not exhibit diauxic growth (Figures S1A and S1B). Surprisingly, A1501 grew very poorly on a citrate/benzoate mixture, and even more slowly on benzoate, implying that benzoate exerts a strong inhibitory effect on citrate utilization (Figure S1C). Conversely, A1501 co-utilized glucose and benzoate, exhibiting a much higher growth performance (the maximal OD_{600} of approximately 1.0) than on each individual source (the maximal OD_{600} of 0.30 and 0.45, respectively) (Figure 1F), as previously described for *Pseudomonas* sp. CSV86 and *E. coli*.[49,50] Together, A1501 preferentially catabolized the top tier substrates succinate and lactate, followed by citrate at a relatively less favorable level, and ultimately the non-preferred substrates glucose and benzoate; however, the sophisticated mechanisms underlying this phenomenon remain to be investigated in depth.

Mutation of the *hfq/crc/crcZY* genes and prediction of putative hfq-binding mRNAs

An analysis of the location of the putative regulatory genes controlling carbon catabolite repression in the *P. stutzeri* A1501 genome identified seven genes that are known to be involved in this process in other *Pseudomonas* species[5,9] and revealed a cluster carrying the *cbrAB* genes of the two-component system linked to *crcZ*, while *hfq*, *rpoN*, *crc*, and *crcY* are not linked and belong to different clusters (Figure 2A and Table S2). Single and double mutants were constructed to obtain insights into their biological functions (Figure 2B). Growth with the preferred carbon source lactate or succinate was not impaired in any of the mutant strains, but a similar result was not observed for citrate. Although citrate is generally considered the preferred carbon source of *Pseudomonas*,[9] the *ΔcrcZΔcrcY* double mutation strongly impaired growth on citrate as the sole carbon source (Figure 2B), suggesting that citrate utilization might be subject to carbon catabolite repression in strain A1501. Furthermore, we found that the *ΔcbrA* or *ΔcbrB* single mutants and the *ΔcrcZΔcrcY* double mutant did not grow on two non-preferred carbon sources, glucose or benzoate (Figure 2B), suggesting that these genes play key roles in carbon catabolite repression. The deletion of either *crcZ* or *crcY* had no effect on catabolite repression, suggesting that the two genes may be functionally complementary, as described in *P. putida*.[27] The Δ*crc* mutant exhibited wild-type diauxic growth, whereas the *Δhfq* mutant exhibited the same phenotype defect in diauxie as the *ΔhfqΔcrc* double mutant, suggesting that Hfq has a stronger function than that of Crc in catabolite repression on glucose utilization.

Recent studies revealed that Hfq recognizes a common catabolite activity (CA) motif that contains an AANAANAA motif close to the AUG translation start codon of target mRNAs.[12,14] An analysis of the phenotype of the *hfq* mutant helped identify the possible target genes that are involved in the utilization of non-preferred carbon sources by *P. stutzeri* A1501. Glucose is metabolized by the Entner-Doudoroff pathway in *Pseudomonas* species.[51] The *gltR* gene encodes a transcriptional regulator that interacts with different promoters to regulate the expression of the *oprB*, *glk*, and *edd* genes located in different clusters in the A1501 genome (Figure 2A and Table S2), all of which are required for glucose transport and utilization.[52] As shown in Figure 2C, a CA motif was identified in the mRNAs of these genes required for glucose metabolism. The characterization of the genes involved in benzoate utilization (Figure 2A) was previously reported in *P. stutzeri* A150.[48] An analysis of the mRNA sequences of these genes identified a CA motif in *benR*, *benF*, and *benK* (Figure 2C). Consistent with the hypothesis mentioned above that citrate utilization may also be controlled by catabolite repression, a CA motif was found in the mRNA of the *citN* gene

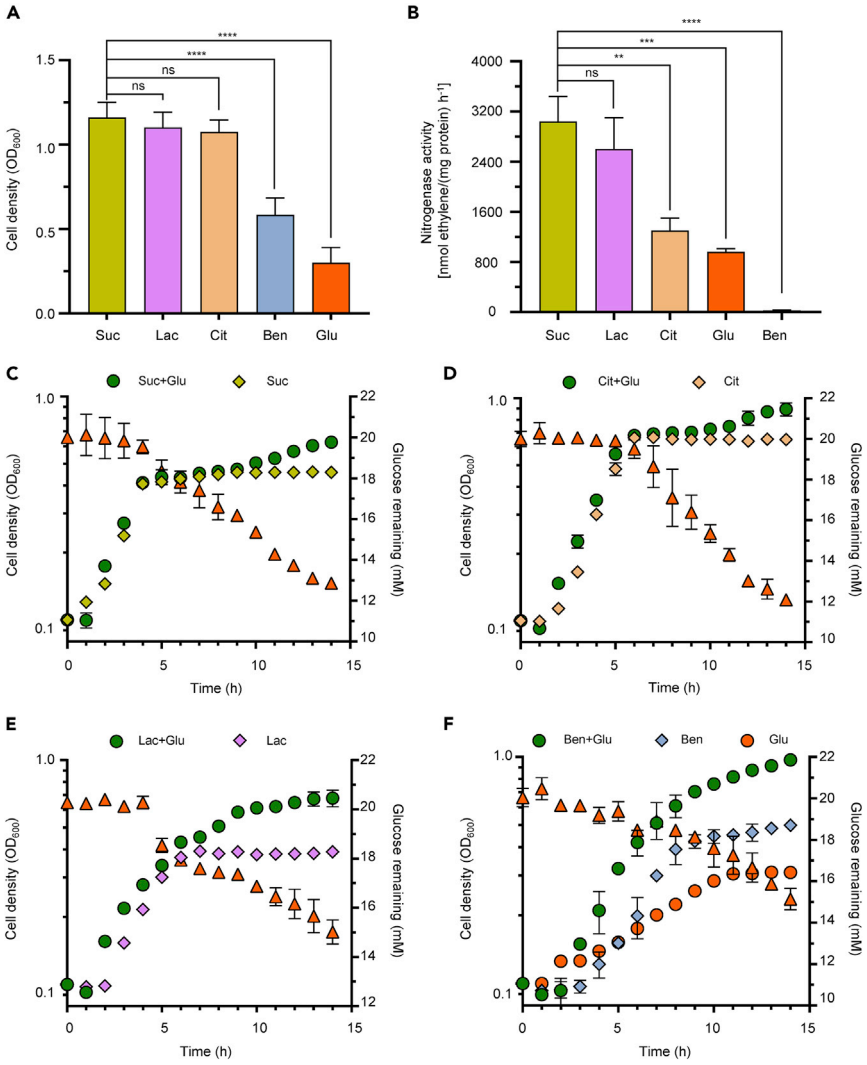

Figure 1. Hierarchical utilization of carbon substrates in *P. stutzeri* A1501

(A) Growth of A1501 for 12 h in minimal medium K that contained 6.0 mM NH_4^+ as the sole nitrogen source and with the carbon sources indicated at the following concentrations: 4 mM benzoate (Ben), 20 mM lactate (Lac), 20 mM succinate (Suc), 20 mM citrate (Cit), and 20 mM glucose (Glu).

(B) Effect of the different carbon substrates on the nitrogenase activity of A1501 in minimal medium K devoid of a nitrogen source and containing the same carbon substrates as in (A).

(C) Diauxic growth of A1501 in minimal medium K supplemented with 6.0 mM NH_4^+ and a mixture of 4 mM Suc plus 20 mM Glu. The growth curve (OD_{600} versus time) is shown together with the measured concentration of glucose remaining in the medium (orange triangles). Growth with succinate alone is shown as a control.

(D and E) Diauxic growth of A1501 under conditions similar to (C) but with 4 mM citrate (D) or 4 mM lactate (E) instead of succinate and controls with citrate and lactate alone.

(F) Growth curve of A1501 on 4 mM benzoate plus 20 mM glucose and controls with glucose and benzoate alone. See Figure S1 for the growth curve of A1501 on benzoate plus succinate or lactate.

Data shown in (A and B) are presented as the means ± SEM (n = 9). Asterisks indicate statistical significance determined using one-way ANOVA with Tukey's post hoc test: ****$p \leq 0.0001$, ***$p \leq 0.001$, **$p \leq 0.01$, and ns: non-significant. Data shown in (C–F) are representative of two independent experiments and are presented as the means ± SEM (n = 6).

encoding a citrate transporter (Figure 2C). These results suggest that Hfq has a major role in regulatory systems underlying hierarchical carbon substrate utilization, similar to those in other *Pseudomonas* species. It was previously reported that an *hfq* mutant strain displayed reduced nitrogenase activity.[46] Most interestingly, a CA motif was also identified in the coding region of the *nifH* mRNA encoding a nitrogenase Fe

A

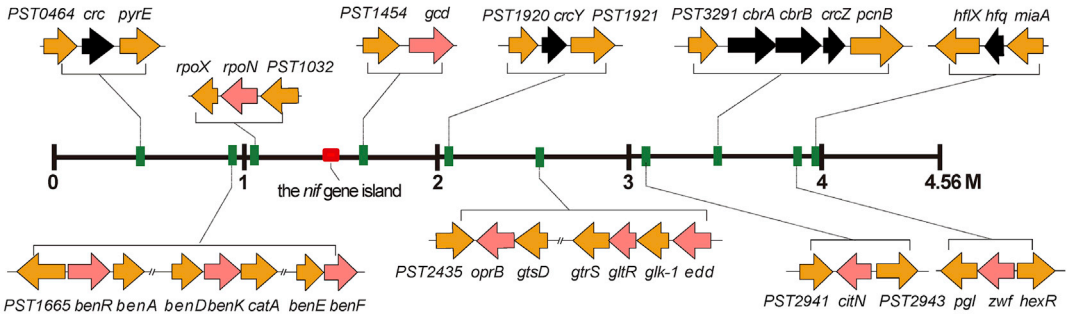

B

Strains[a]	Sole carbon source[b]					Mixed carbon source[c]			LB
	Lac	Suc	Cit	Glu	Ben	Lac + Glu	Suc + Glu	Ben + Glu	
A1501	++	++	++	+	+	++	++	++	+++
Δ*cbrA*	++	++	++	-	-	++	++	-	+++
Δ*cbrA* (p*cbrA*)	++	++	++	+	+	++	++	+	+++
Δ*cbrB*	++	++	++	-	-	++	++	-	+++
Δ*cbrB* (p*cbrB*)	++	++	++	+	+	++	++	++	+++
Δ*crc*	++	++	++	+	+	++	++	+	+++
Δ*crc* (p*crc*)	++	++	++	+	+	++	++	++	+++
Δ*hfq*	++	++	++	+	+	++, ×	++, ×	+	+++
Δ*hfq* (p*hfq*)	++	++	++	+	+	++	++	++	+++
Δ*hfq/crc*	++	++	++	+	+	++, ×	++, ×	+	+++
Δ*hfq/crc* (p*hfq*)	++	++	++	+	+	++	++	++	+++
Δ*hfq/crc* (p*crc*)	++	++	++	+	+	++, ×	++, ×	+	+++
Δ*crcY*	++	++	++	+	+	++	++	++	+++
Δ*crcY* (p*crcY*)	++	++	++	+	+	++	++	++	+++
Δ*crcZ*	++	++	++	+	+	++	++	++	+++
Δ*crcZ* (p*crcZ*)	++	++	++	+	+	++	++	++	+++
Δ*crcY/crcZ*	++	++	-	-	-	++, ×	++, ×	-	+++
Δ*crcY/crcZ* (p*crcY*)	++	++	++	+	+	++	++	++	+++
Δ*crcY/crcZ* (p*crcZ*)	++	++	++	+	+	++	++	++	+++
A1501 (pLAFR3)[d]	++	++	++	+	+	++	++	++	+++

C

gltR	5' - AAGGCGACGGGCGAUCGGAUAACAACAAGAAAAGGGACGUGACGUGAGCCAAGCAGG
zwf	5' - UCAUAGUGCAGUGUUAGUAGAAGAACAAACAUCAUGACGCCAUUAUCUGUCGAACCCU
oprB	5' - ACAGGCUCGAUCCAGCGAUCAAUAACAACAAAAGCGGAGUGGAUAUGAAAAAAAC
edd	5' - CGGAUGGUUUAUGGUUGUCGAAGAACAAAAUUCCGCAGCAGGAGAGACGCAUGCAC
gcd	5' - UCUGGAAUGUGUGCAGGUCGAACAACAAGAGCGAGGAGUUGGCGCCGUGGCAGUAG
benF	5' - GCGGCUGCGUGCACCCUGAAAACAACAACAAGAGAGUUAGAUGAUGCAGAAGGUAUC
benK	5' - GCUGCAGCCGAUCCGCGACUAACAAAAACAAUAGAGAGUCUUGCCAUGCGAAAAGUA
benR	5' - CACUAAGCGCCGCCAACUAUAAAAACAACCGAGUGCCGGGUGAUGGAACGACUGCUG
citN	5' - CCCUGCUGCUUCGGCCGGACAAGAAUAAAGAGGAGGUAAGCUGUGUUGACCCUGAUU
nifH	5' - UGAGGAACUUAAUUAUGG…GAACAAGAAACUGGUCAUCCCCACCCCGAUCAGCAUGG

Figure 2. Systematic investigation of genes involved in carbon catabolite repression and sequence alignment of putative Hfq-binding mRNAs containing a CA motif

(A) Localization of the gene clusters on a linear map of the chromosome. See also Table S2 for a functional description of the *cbrAB*/*hfq*/*crc*/*crcZ*/*crcY* genes and corresponding substrate-specific catabolic genes. Black arrows indicate genes of interest that were inactivated by homologous suicide plasmid integration using pK18mob as a vector in this study.

(B) Analysis of the growth characteristics of *P. stutzeri* A1501, the corresponding mutant, and complemented strains. [a] Growth was tested in K medium supplemented with a single carbon source or mixed carbon sources, as indicated, at 30°C after 12 h. In minimal medium K containing 6 mM NH_4^+ and 20 mM lactate, the growth performance of the mutant strains was similar to that of the wild-type A1501; [b] Suc, 20 mM succinate; Lac, 20 mM lactate; Cit, 20 mM citrate; Glu, 20 mM glucose; Ben, 4 mM benzoate; [c] Lac + Glu, 4 mM lactate plus 20 mM glucose; Suc + Glu, 4 mM succinate plus 20 mM glucose; Ben + Glu, 4 mM benzoate plus 20 mM glucose. [d] Empty vector control. +++, Maximal growth ($OD_{600} \geq 2.0$); ++, moderate growth ($2.0 > OD_{600} > 0.5$); +, weak growth ($0.5 > OD_{600} > 0.15$); -, no growth ($OD_{600} < 0.15$); ×, mutation that completely abolishes the diauxic growth pattern. Experiments were performed three times with similar results.

(C) The CA motif located at the 5′ untranslated region close to the translation start site of substrate-specific catabolic gene mRNAs and the coding region of the nitrogenase Fe protein gene *nifH* mRNA. Sequences of CA motifs are highlighted in yellow. The putative ribosome-binding site (RBS) is underlined. The initiation codon is indicated in red.

protein, probably as a putative target for Hfq, suggesting that Hfq-mediated control is not limited to carbon source utilization.

Involvement of hfq and crc in the organic acid-mediated carbon catabolite repression

To further assess the contribution of the *hfq* and *crc* genes to carbon catabolite repression, we first used droplet digital PCR (ddPCR) to measure their absolute transcription levels under conditions that generated strong catabolite repression. During diauxic growth of the wild type in a medium containing both succinate and glucose, as shown in Figure 3A, the *hfq* mRNA level was rapidly upregulated at the first growth phase and then downregulated remarkably during the second growth phase; in contrast, the *crc* mRNA level was very low and remained unchanged during both growth phases. During the first exponential growth phase in which the abundance of *hfq* mRNA was high, the glucose concentration in the culture medium barely changed, suggesting the necessity of Hfq for catabolite repression of glucose utilization. Under the same growth conditions, the *Δcrc* mutant exhibited a pattern of biphasic growth, similar to that of the wild-type strain (Figure 3B), whereas the *Δhfq* or *ΔhfqΔcrc* mutant strains showed no diauxie (Figures 3C and 3D), suggesting that carbon catabolite repression was not abolished by deleting Crc. These findings suggest that the presence of Hfq may be necessary and sufficient for catabolite repression, as reported first in *P. aeruginosa*.[20]

In *P. aeruginosa*, unlike Hfq, Crc was not found to bind CA motifs but to have an auxiliary function in Hfq-mediated repression.[14,15] Thus, we used microscale thermophoresis (MST) to analyze the ability of both Hfq and Crc proteins to recognize predicted CA motifs in the 5′ untranslated region of the target genes, including the *gltR*, *oprB*, *edd* and *zwf* genes responsible for glucose utilization, the *benR* gene encoding a transcriptional activator for the benzoate degradation pathway, and the *citN* gene encoding a citrate transporter. As revealed in Figures 3E, 3G, 3I, 3K, and 3M (green curve), Hfq directly bound to each of the wild-type mRNAs. The same experiments were reproduced using mutated mRNAs devoid of the CA motif to support these data, and the ability to bind Hfq was lost (Figures 3E, 3G, 3I, 3K, and 3M, red curve). In the presence of Crc, the binding of Hfq to target mRNAs was significantly enhanced (Figures 3F, 3H, 3J, 3L, and 3N). However, in the absence of Hfq, no binding of Crc to wild-type mRNAs was observed (Figure S2). The oligonucleotides that contained the 5′-UTR and the full-length coding region of the indicated mRNAs used for MST analysis and sequences of the WT or mutated CA motif are summarized in Figure 3O.

Other experiments were performed using strains carrying translational *lacZ* fusions to the *gltR* and *edd* genes. Measurement of *in vivo* β-galactosidase activity in a medium containing both succinate and glucose showed increased activities when the fusions were introduced into the Δ*hfq* and Δ*crc* mutant strains, but this increase was eliminated by genetic complementation with a plasmid carrying the wild-type *hfq* and *crc* genes (Figure S3). These *in vivo* experiments further support the hypothesis that Hfq and Crc act in a coordinated manner to mediate the repression of the genes required for glucose utilization at the translation level.

CrcZ antagonizes hfq-mediated translational repression of non-preferred catabolic pathways

CrcZ and CrcY levels were reported to vary widely based on the carbon source used in *P. aeruginosa* and *P putida*.[53,54] In the present study, the level of *crcZ* is low under conditions causing strong catabolic

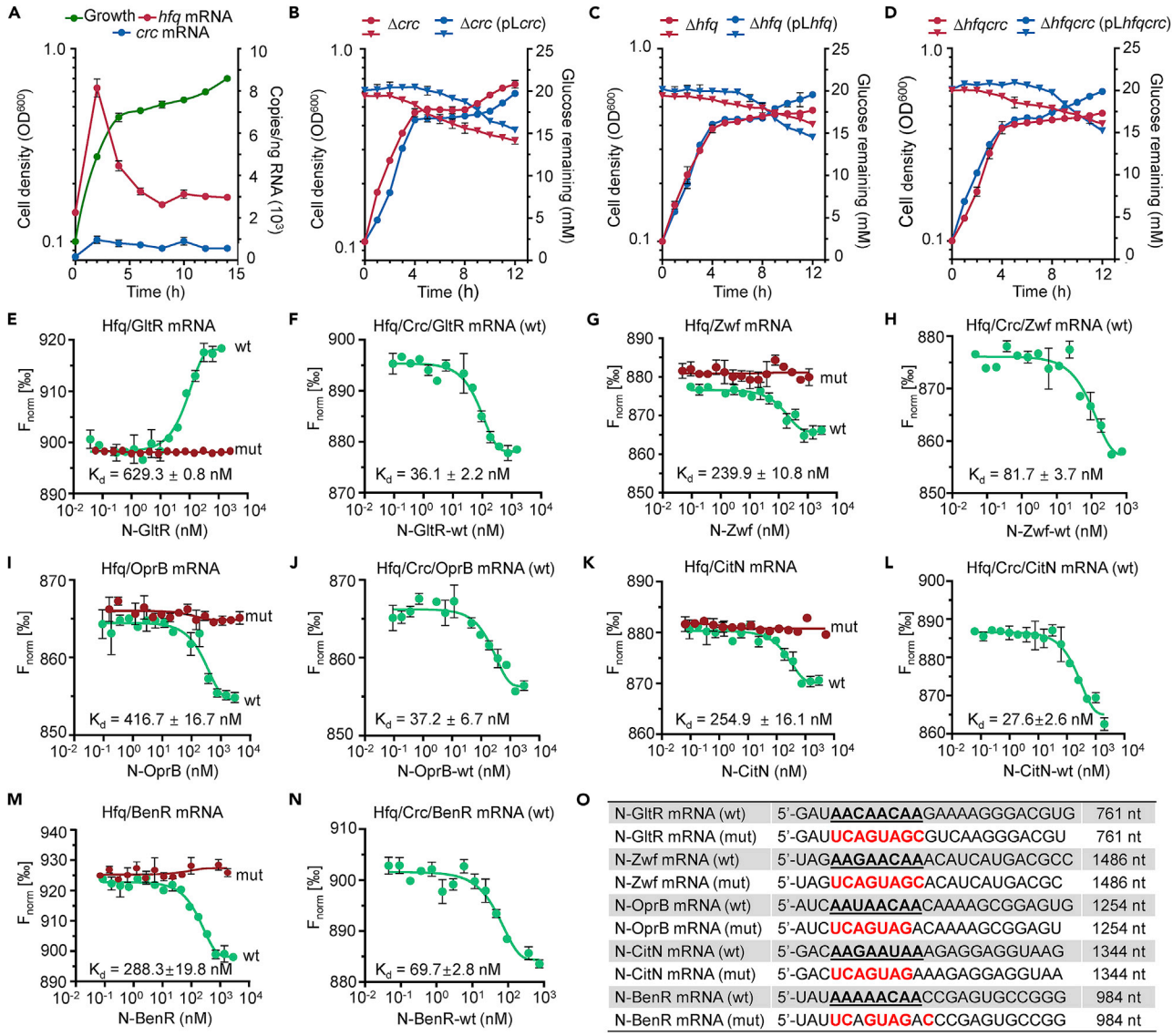

O

N-GltR mRNA (wt)	5′-GAU**AACAACAA**GAAAAGGGACGUG	761 nt
N-GltR mRNA (mut)	5′-GAU**UCAGUAGC**GUCAAGGGACGU	761 nt
N-Zwf mRNA (wt)	5′-UAG**AAGAACAA**ACAUCAUGACGCC	1486 nt
N-Zwf mRNA (mut)	5′-UAG**UCAGUAGC**ACAUCAUGACGC	1486 nt
N-OprB mRNA (wt)	5′-AUC**AAUAACAA**CAAAAGCGGAGUG	1254 nt
N-OprB mRNA (mut)	5′-AUC**UCAGUAG**ACAAAAGCGGAGU	1254 nt
N-CitN mRNA (wt)	5′-GAC**AAGAAUAA**AGAGGAGGUAAG	1344 nt
N-CitN mRNA (mut)	5′-GAC**UCAGUAG**AAAGAGGAGGUAA	1344 nt
N-BenR mRNA (wt)	5′-UAU**AAAAACAA**CCGAGUGCCGGG	984 nt
N-BenR mRNA (mut)	5′-UAU**UCAGUAGA**CCCGAGUGCCGG	984 nt

Figure 3. Hfq and Crc act as translational repressors of substrate-specific catabolic genes

(A) Absolute numbers of copies of the *hfq* and *crc* mRNAs during diauxic growth of WT A1501 on 4 mM succinate plus 20 mM glucose.

(B–D) Growth of the Δ*crc* (B), Δ*hfq* (C), Δ*hfq*Δ*crc* (D) mutant strains (red) and their corresponding complemented strains (blue) that were grown on 4 mM succinate plus 20 mM glucose. The growth curve (circle) is shown together with the measured concentration of glucose (triangle) remaining in the medium.

(E–N) Determination of the binding affinity of labeled Hfq for the target mRNAs containing the WT or mutated CA motifs in the absence and presence of 400 nM Crc. Ligand-dependent changes in MST are plotted as normalized fluorescence (F_{norm}) values vs. ligand concentration in a dose-response curve. F_{norm} values are plotted as parts per thousand [‰] for binding affinity analysis. N: ssRNA oligonucleotides; wt: wild-type; mut: mutant.

(O) The WT or mutated oligonucleotides that contained the 5′-UTR and the full-length coding region of the indicated mRNAs were used for MST analysis. Sequences of the CA motif (AAnAAnAA) are shown in boldface and underlined. Point mutations introduced into synthesized oligonucleotide derivatives are shown in red. N, ssRNA oligonucleotide; wt, wild type; mut, mutation.

Data shown in (A–N) are representative of two independent experiments and are presented as means ± SEM (n = 6). See also Figures S2 and S3.

repression, but increases substantially in the presence of glucose or benzoate as the sole carbon source (Figure 4A). Notably, the level of *crcZ* is also moderately increased during growth with citrate as a sole carbon source (Figure 4A), providing a possible explanation for the growth defect of the *ΔcrcZΔcrcY* double mutant on citrate (Figure 2B). During diauxic growth in the presence of succinate plus glucose, CrcZ levels increase sharply during the transition from the first exponential phase to the second (Figure 4B), suggesting that this ncRNA may be essential for abrogating Hfq-mediated translational repression. Unlike *crcZ*, the level of *crcY* is very low and remains virtually unchanged, regardless of the carbon source used under all

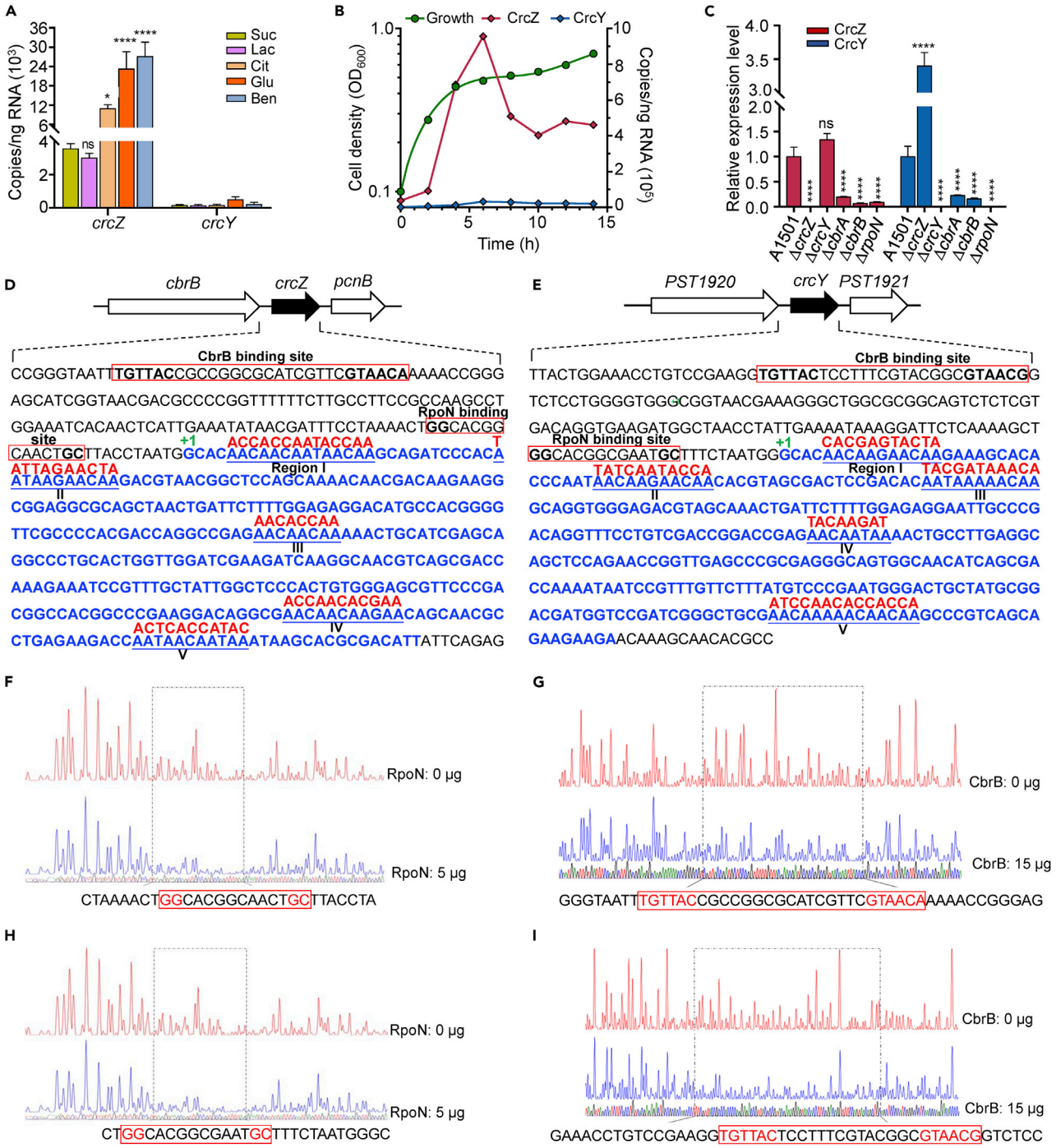

Figure 4. Functional analysis of the regulatory ncRNAs CrcZ and CrcY

(A) Absolute levels of the *crcZ* and *crcY* transcripts in strain A1501 grown on succinate and other carbon substrates. Bacteria were grown in minimal medium Kcontaining 6.0 mM NH_4^+ and supplemented with 20 mM lactate (Lac), succinate (Suc), citrate (Cit), and glucose (Glu) and 4 mM benzoate (Ben). A 4 h incubation time was chosen for droplet digital PCR (ddPCR) assays. The absolute transcript level is reported as the number of copies per ng of total RNA. Means ± SEM (n = 6) are shown. Asterisks indicate statistical significance determined using two-way ANOVA with Tukey's post hoc test: ****p ≤ 0.0001, *p ≤ 0.05, and ns: non-significant.

(B) Changes in absolute levels of the *crcZ* and *crcY* transcripts during diauxic growth. Bacterial cells were incubated in minimal medium K containing 6.0 mM NH_4^+ supplemented with a mixture of 4 mM succinate and 20 mM glucose, and samples were collected at regular intervals (0, 2, 4, 6, 8, 10, 12, and 14 h) for ddPCR assays. Data are representative of two independent experiments and are presented as the means ± SEM (n = 4).

Figure 4. *Continued*

(C) Relative levels of the *crcZ* and *crcY* transcripts on wild-type and mutant backgrounds under the same growth conditions as in (B), which were measured using qRT-PCR. Means ± SEM (n = 9) are shown and asterisks indicate statistical significance determined using two-way ANOVA with Tukey's post hoc test: ****p ≤ 0.0001 and ns: non-significant.

(D and E) Genetic organization of the *crcZ* (D) or *crcY* (E) regions in the *P. stutzeri* A1501 chromosome. The putative CbrB- or RpoN-binding sites are marked by red boxes. +1 indicates the transcription start site based on a 5′ RACE analysis. The nucleotide sequences of the *crcZ* and *crcY* genes are indicated in boldface. Both ncRNAs have five unpaired A-rich regions (shown underlined) containing putative CA motifs to which Hfq can potentially bind. Point mutations were introduced into the synthesized oligonucleotide that was used for the MST analysis (see Figure S5), and the corresponding mutated sequences (indicated in red) are shown above the unpaired region.

(F–I) DNase I footprinting analysis of the *crcZ* (F, G) and *crcY* (H, I) promoter probes using purified RpoN protein added at 0 and 5.0 μg or purified CbrB protein added at 0 and 15 μg. The RpoN- or CbrB-protected region is indicated by a dotted box, with the nucleotide sequence shown at the bottom. The RpoN- and CbrB-binding sites are marked by red boxes.

See also Figures S4 and S5.

conditions tested (Figures 4A and 4B), implying that CrcY does not appear to play a role in adjusting the strength of catabolite repression. However, the deletion of either *crcZ* or *crcY* led to a compensatory increase in the levels of the remaining ncRNA, as also observed in *P. putida*.[27] For example, the levels of *crcY* in the strain lacking *crcZ* increased more than 3.0-fold compared to the wild-type strain (Figure 4C). This result may explain why the single deletion of *crcZ* or *crcY* had no effect on catabolite repression, but the double mutation resulted in constitutive catabolite repression that compromised the growth of citrate or glucose (Figure 2B). In particular, the level of CrcY was upregulated by about 13.4- and 4.5-fold at high temperature (45°C) or in the presence of saline stress, in contrast to CrcZ, whose expression was upregulated by approximately 2.2-fold under nitrogen fixation conditions (Figure S4), suggesting a CrcZY-mediated regulatory link between environmental stresses and carbon/nitrogen metabolism.

In addition, we found that the single deletion of the *cbrA*, *cbrB*, or *rpoN* genes caused a significant decrease in the expression levels of *crcZ* and *crcY* (Figure 4C), consistent with observations in other *Pseudomonas* strains.[26,55] The position of the transcription start site for the promoters of both *crcZ* and *crcY* was determined by 5′RACE (Figures 4D and 4E). Further inspection of the DNA regions located upstream from the promoters of *crcZ* and *crcY* revealed the presence of conserved sequences (at position −24/-12) typical of a RpoN-dependent promoter and a putative CbrB binding site (Figures 4D and 4E), suggesting that both RpoN and CbrB controlled the expression of *crcZ* and *crcY*. This hypothesis was confirmed by DNase I footprinting assays (Figures 4F-4I). Both ncRNAs are predicted to contain five unpaired A-rich regions with putative CA motifs to which Hfq potentially binds (Figures 4D and 4E). A set of full-length CrcZ and CrcY ssRNA oligonucleotides containing the WT sequences (N-CrcZ-wt and N-CrcY-wt) and mutated sequences (the N-CrcZ-mut2 and N-CrcY-mut2 containing site-specific mutations in regions II and V, and the N-CrcZ-mut5 and N-CrcY-mut5 containing site-specific mutations in all five regions) were synthesized for the MST analysis to obtain experimental evidence for the predicted interactions between Hfq and CrcZ and CrcY individually (Figures 4D and 4E). As anticipated, both CrcZ and CrcY directly bind to Hfq, exhibiting Kd values of 23.7 ± 2.68 nM and 22.21 ± 4.68 nM, respectively (Figures S5A and S5D). The binding was significantly weakened or was even completely lost if the CA motif was mutated (Figures S5B, S5C, S5E, and S5F). Taken together, these experiments showed that the regulatory ncRNA CrcZ acts as a key decoy to antagonize Hfq-mediated translational repression of the catabolic genes necessary for the consumption of non-preferred carbon sources.

Hfq optimizes root-associated nitrogenase activity via positive regulation of *nifA* and *nifH* expression at the transcriptional and translational levels

Under laboratory conditions, nitrogenase activity associated with host seedlings or roots, which is usually low due to the limited carbon supply from root exudates, has been reported to increase after the addition of carbon sources.[56,57] This result was also observed in rice roots inoculated with A1501 where no root-associated nitrogenase activity was detected in the absence of an additional carbon source; therefore, this condition was chosen as a negative control (Figure 5A). Interestingly, the root-associated nitrogenase activity of A1501 incubated with succinate was increased up to 12,000 U, which was approximately 3-fold higher than the nitrogenase activity of A1501 in the free-living state, and 6-fold higher than the root-associated nitrogenase activity of A1501 grown on glucose (Figure 5A), indicating that nitrogenase activity was significantly increased in the presence of roots, or more precisely certain root exudates. Next, acetylene reduction assays were performed with mutant strains using the same conditions as with the wild type. Inoculation with *ΔcrcZ* or *ΔcrcY* strains had little effect, while the inoculation of strains carrying *Δcrc*, *Δhfq* or

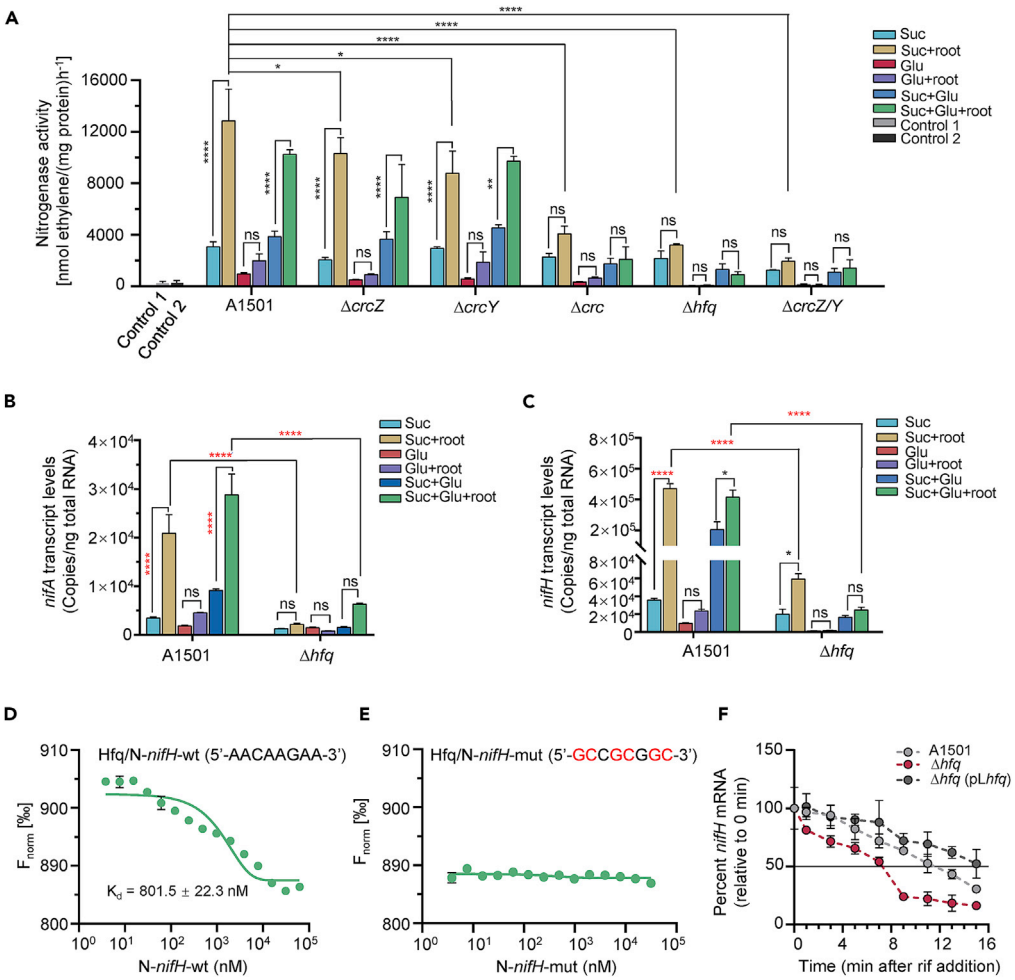

Figure 5. Hfq exerts a positive regulatory effect on root-associated nitrogenase activity at the transcriptional and translational levels

(A) Nitrogenase activity assays using wild-type and mutant strains associated with or without rice roots in the presence of 4 mM succinate (Suc) and 20 mM glucose (Glu) alone or in combination. Control 1: Rice roots without inoculation; Control 2: rice roots inoculated with A1501 but without an additional carbon source.

(B and C) The absolute copy numbers of the *nifA* mRNA (B) and *nifH* mRNA (C) under the same conditions as in (A), which were determined using ddPCR.

(D and E) Determination of the binding affinity of labeled Hfq to *nifH* mRNA containing the WT (D) or mutated CA motif (E) using microscale thermophoresis. The CA motifs are shown in parentheses, and point mutations introduced into a synthesized oligonucleotide are shown in red. N, ssRNA oligonucleotide; wt, wild type; mut, mismatch mutation.

(F) Analysis of the *nifH* mRNA half-life in the WT and *hfq* mutant strains. Rifampicin (400 μg/mL) was added at time 0. At the indicated times, an equal volume of frozen media was added to bring the temperature immediately to 4°C. RNA was extracted, followed by qRT-PCR.

Data shown in (A–C) are representative of two independent experiments and are presented as means ± SEM (n = 4). Asterisks indicate statistical significance determined using two-way ANOVA with Tukey's post hoc test: ****$p \leq 0.0001$, ***$p \leq 0.001$, **$p \leq 0.01$, *$p \leq 0.05$, and ns: non-significant. Data shown in (D–F) are presented as the means ± SEM (n = 6).

ΔcrcZY mutations led to a significant decrease in root-associated nitrogenase activities, especially in the presence of mixed carbon sources (Figure 5A).

Knockout of *hfq* has also been reported to decrease the abundance of the *nifH* mRNA encoding a subunit of the nitrogenase, as well as the *nifA* mRNA, encoding a transcriptional activator of all *nif* operons in *Azorhizobium caulinodans*[58] and *Sinorhizobium meliloti*.[59] This is why we measured the *nifA* and *nifH* mRNA levels of wild-type and *hfq* mutant strains associated with roots using droplet digital PCR (ddPCR).

Consistent with the results shown in Figure 5A, an order of magnitude increases in the absolute copy number of both *nifH* and *nifA* mRNAs was observed when bacteria were grown on succinate or a mixture of glucose with rice roots compared with the level obtained without roots (Figures 5B and 5C, red asterisks indicate statistically significant differences). Mutation of *hfq* suppressed this stimulatory effect; for example, the absolute copy number of both *nifH* and *nifA* mRNAs in the *hfq* mutant decreased by more than 3.0- or 30.0-fold compared with the wild-type strain (Figures 5B and 5C), suggesting that Hfq exerts a positive regulatory effect on the expression of both genes in bacteria associated with roots. In addition, consistent with previous observations showing that the use of glucose as a sole carbon source poorly supports nitrogen fixation (Figure 1B), this non-preferred carbon source has no effect on the expression of both *nifH* and *nifA* mRNAs (Figures 5B and 5C). Moreover, *nifH* is the only gene among all the *nif* genes to contain the CA motif in its mRNA, suggesting that it is the target of Hfq (Figure 2C). As expected from MST experiments, Hfq directly binds to the CA motif located in the *nifH* coding region, while mutating this motif led to a complete lack of binding to Hfq (Figures 5D and 5E). We subsequently measured the half-life of the *nifH* transcript, which was 10.5 min for the WT and 7.0 min for the Δ*hfq* mutant (Figure 5F), indicating that Hfq exerted a positive effect on the stability of the *nifH* mRNA.

Involvement of *hfq*/*crc*/*crcZY* genes in root colonization via the transcriptional regulation of exopolysaccharide production

A1501 exhibited poor growth on glucose but high respiratory activity (Figure 1F and Table S1); thus, we hypothesized that glucose is rapidly utilized not as a growth substrate but as a precursor to produce exopolysaccharides, which have been shown to be important for colony morphology and root colonization.[60–62] Colony morphology was examined after seven days of growth with succinate and glucose alone or in combination. A1501 exhibited an opaque, wrinkled colony morphology after being grown on dual carbon sources, and this colony was much larger than the colony formed on each substrate alone (Figure 6A), which correlated with the amount of exopolysaccharides produced (Figure 6B). Wild-type phenotypes were totally abolished by the inactivation of the *hfq*/*crc*/*crcZY* genes (Figure 6B), suggesting their involvement in colony morphology and exopolysaccharide production. Consistent with the function of *pslA*, the first gene in the *psl* operon that is involved in the synthesis of Psl exopolysaccharide in *P. aeruginosa*[63] and *P. stutzeri*,[64] the *pslA* mutant grown on mixed carbon sources not only produced fewer exopolysaccharides but formed colonies much smaller than those of the WT strain (Figures 6A and 6B). Unexpectedly, the Δ*glk* mutant formed colonies very similar to the WT strain (Figure 6A) while producing more exopolysaccharides than the other mutants, suggesting that sugar nucleotide precursor synthesis in A1501 used a pathway independent of the *glk* gene. In addition, the production of exopolysaccharides is important for biofilm formation and root surface colonization.[60,64] Here, *pslA* expression was significantly increased by approximately 33-fold after exposure to glucose in the presence of roots (Figure 6C). Sugar nucleotide precursors for exopolysaccharide production are generally synthesized from glucose-6-P dependent on glucokinase, which is encoded by the *glk* gene in *Pseudomonas*.[65] When grown on a mixture of 3 mM glucose plus succinate, increasing the concentrations of glucose from 0.4 mM to 3.0 mM led to a continued increase in both *pslA* expression and exopolysaccharide production (Figures 6D and 6E). These results suggest that exopolysaccharide production depends on an adequate supply of glucose but is not inhibited by succinate.

Furthermore, we tested the effect of different concentrations of glucose on root surface colonization by A1501. As shown in Figure 6F, the level of colonization in the presence of 0.2 mM glucose was 2.7 times higher than that in the absence of glucose, indicating that glucose promotes root colonization. However, higher concentrations of glucose resulted in partial or total loss of the stimulatory effect (Figure 6F). We performed co-culture and co-inoculation assays using A1501 and its mutant derivatives to test the roles of the *hfq*/*crc*/*crcZY* genes. In both types of experiments, the individual mutants were recovered at significantly lower levels than A1501, suggesting a competitive disadvantage (Figures 6G and 6H). The Δ*hfq* mutant was reduced to a minor fraction of the total bacteria (less than 0.1%) isolated from co-culture (Figure 6G) or from rice roots (Figure 6H), suggesting that Hfq is crucial for root surface colonization. Quantitative RT-PCR experiments were performed to compare the expression of the *psl* genes during root surface colonization. As shown in Figure 6I, the deletion of *hfq* resulted in a significant decrease in the expression of all *psl* genes, suggesting indirect Hfq-mediated regulation since the mRNAs of these genes do not contain the putative CA motif. These data indicate a crucial role for Hfq in root surface colonization through the positive regulation of *psl*-like genes that are required for Psl production.

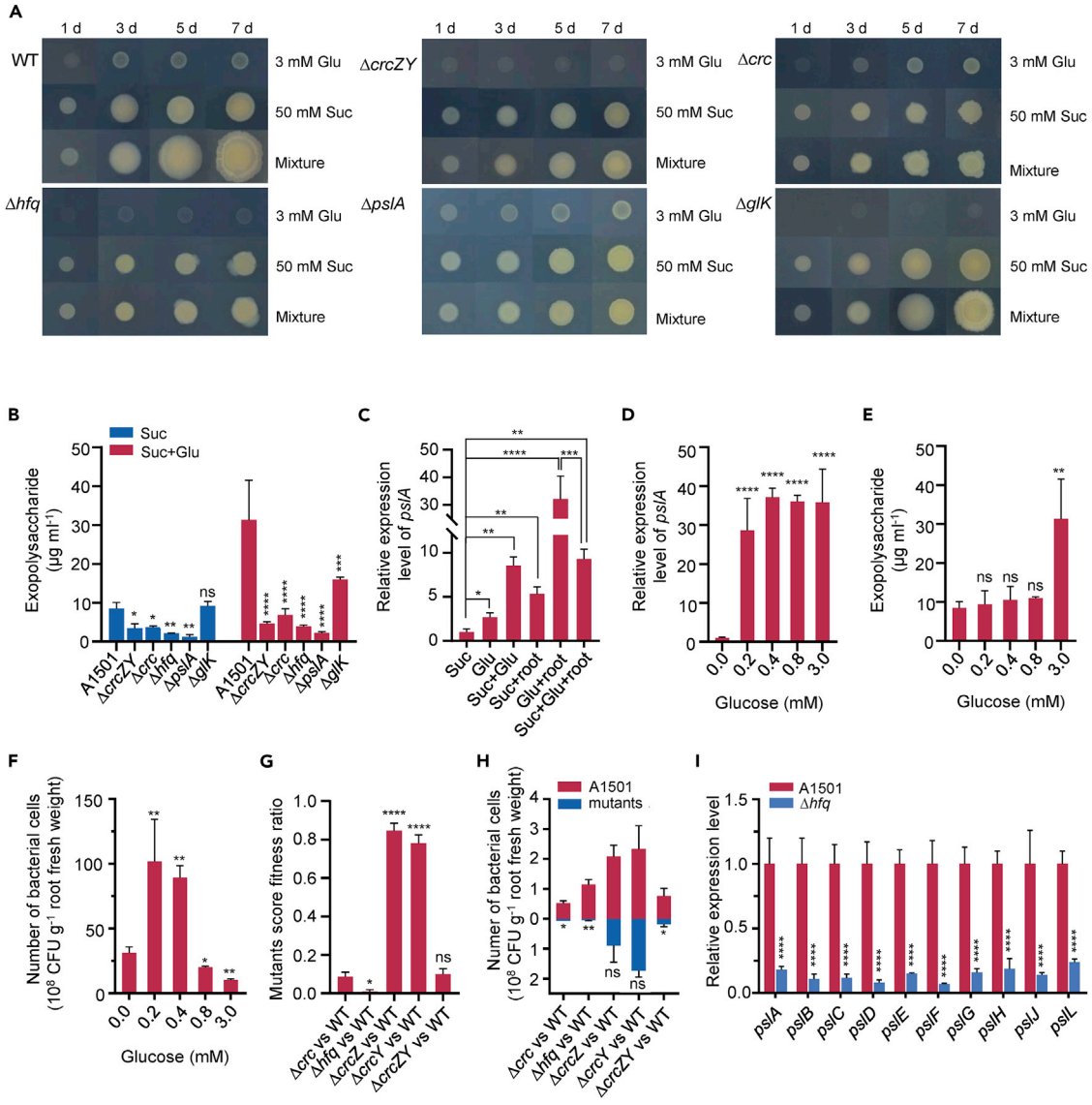

Figure 6. The contribution of *hfq*/*crc*/*crcZY* genes to improving root colonization

(A) The colony morphology of WT and mutant strains was evaluated on minimal medium K that was supplemented with different carbon sources during the 7-day incubation period. Images were taken with the same magnification.

(B) Effect of gene mutations on exopolysaccharide production. Suc, succinate at 50 mM; Glu, glucose at 3 mM. Asterisks indicate statistical significance determined using two-way ANOVA with Tukey's post hoc test: ****p ≤ 0.0001, ***p ≤ 0.001, **p ≤ 0.01, *p ≤ 0.05, and ns: non-significant.

(C) Relative expression levels of *pslA* in A1501 grown on various carbon substrates in the presence or absence of rice roots, as measured using qRT-PCR.

(D) Effect of different concentrations of glucose on the transcription of *pslA* in A1501 grown on minimal K medium supplemented with 6 mM NH_4^+ and 50 mM succinate. Asterisks indicate statistical significance determined using one-way ANOVA with Tukey's post hoc test: ****p ≤ 0.0001.

(E) Effect of different concentrations of glucose on exopolysaccharide production by A1501 grown under the same conditions as in (D). Asterisks indicate statistical significance determined using one-way ANOVA with Tukey's post hoc test: **p ≤ 0.01 and ns: non-significant.

(F) The effect of different glucose concentrations on root colonization by A1501 was determined by counting colony-forming units (CFUs) per g of root. Asterisks indicate statistical significance determined using one-way ANOVA with Tukey's post hoc test: **p ≤ 0.01 and *p ≤ 0.05.

(G) Strain competition experiments. The fitness deficit of the test mutants was shown by co-culturing each mutant with wild-type A1501 mixed in a 1:1 ratio, inoculated at a starting OD_{600} = 0.1 and grown for 24 h in LB. At 24 h, cultures were serially diluted and plated on LB plates containing the relevant antibiotics to enable counting of each strain. The wild-type strain was used as the competitor in all experiments. Asterisks indicate statistical significance determined using one-way ANOVA with Tukey's post hoc test: ****p ≤ 0.0001, *p ≤ 0.05, and ns: non-significant.

(H) Competitive root colonization experiments. Rice seedlings were co-inoculated with the test mutant and wild-type A1501. After 24 h of incubation, root samples were collected, and the number of CFUs per g root was determined. The red bars represent the percentage of colonies recovered from the tested

Figure 6. *Continued*

strains; the blue bars represent the percentage of colonies recovered from the competitor (wild-type) strain. Asterisks indicate statistical significance determined using two-tailed unpaired t-tests: **p ≤ 0.01, *p ≤ 0.05, and ns: non-significant.

(I) Quantitative RT-PCR analysis of the transcriptional activities of *psl*-like genes in the wild-type and Δ*hfq* mutant strains during root colonization. Measurements were normalized to the wild-type values, and fold differences are plotted.

Data are the means and standard deviations of three independent experiments. Asterisks indicate statistical significance determined using two-way ANOVA with Tukey's post hoc test: ****p ≤ 0.0001.

DISCUSSION

Carbon source utilization is a typically sequential process that involves external nutrient signaling, followed by transporter-mediated uptake, and ultimately enzymatic catabolism.[17,23] The induction of carbon substrate-specific metabolic pathways depends on the combined activity of specific regulators and node enzymes, some of which are subject to carbon catabolite repression. In the present study, we observed that A1501 preferentially catabolized the top tier succinate and lactate substrates, followed by relatively less favorable substrate citrate, and ultimately the non-preferred substrates glucose and benzoate. Furthermore, genetic data show that carbon catabolite repression operates at mRNAs of various genetic elements required for glucose utilization, including *gltR* encoding a transcriptional regulatory protein, *oprB* encoding a carbohydrate porin, and *zwf* encoding a glucose-6-phosphate dehydrogenase (Figure 3). These findings provide a plausible explanation for why glucose is the most non-preferred carbon source for A1501. In addition, citrate is generally considered the preferred carbon source in *Pseudomonas*,[9] as observed for A1501, which preferentially utilized citrate over glucose. The observation that citrate does not support the growth of the *ΔcrcZΔcrcY* double mutant remain puzzling; thus, citrate exhibits the characteristics of a typical non-preferred carbon source (Figure 2B). This result might be explained by the fact that Hfq binds to the A-rich motif of the *citN* mRNA encoding a citrate transporter (Figure 3K) while citrate moderately induces the expression of CrcZ (Figure 4A). The subject of most interest is benzoate, a derivative of lignin compounds and an intermediate in the catabolism of other aromatic compounds, which substantially inhibits growth and nitrogenase activity but increases the growth rate of glucose (Figure 1). The presumable explanation for this finding is that benzoate induced more CrcZ expression than glucose (Figure 4A), thus effectively relieving the inhibitory effect of Hfq on glucose utilization. Another explanation for our observations is that benzoate exerts a toxic effect on growth, and thus A1501 must evolve specifically adaptive regulatory mechanisms in a rhizosphere environment rich in aromatic carbon sources, as reported for the hegemonic preference of *Cupriavidus pinatubonensis* for benzoate.[66] Therefore, this study provides a framework for understanding the molecular mechanism of hierarchical carbon substrate utilization in *Pseudomonas*. A complex model controlling this hierarchy is summarized in Figures 7 and S6.

The rhizosphere is a hotspot for mutualistic interactions between microorganisms and host plants.[67–69] In particular, plant roots secrete large amounts of carbon-rich compounds into the rhizosphere, including organic acids (succinic, citric, and lactic acids, among others), carbohydrates (glucose, fructose, and so forth), and phenolics (benzoate, benzoxazinoid, and so forth), which can be utilized as carbon and energy sources by root-colonizing pseudomonads.[37,40] The metabolism of root exudates is controlled in a hierarchical manner by a complex regulatory system, including multiple RNA-binding proteins and ncRNAs at the posttranscriptional level.[29] However, questions remain as why root-colonizing pseudomonads would adopt a complex strategy, as well as its physiological and adaptive advantages. In this study, ddPCR experiments quantitatively indicated that Hfq and CrcZ levels vary according to the nature of the carbon sources being used, a phenomenon that was also observed for *P. aeruginosa*,[26] *P. putida*,[27] and *A. vinelandii*.[70] In particular, the abundance of Hfq increased rapidly under conditions that provoked strong repression by succinate (Figure 3A), whereas the synthesis of the ncRNA CrcZ was remarkably increased under non-repressing conditions (Figure 4A). These opposite expression patterns of Hfq and CrcZ, together with the fact that the Crc and CrcY levels are very low, regardless of the carbon source used, underscore the roles of Hfq and CrcZ as a key translational repressor and antagonist pair in carbon catabolite repression. Indeed, this posttranscriptional regulation has physiological advantages, which may allow *Pseudomonas* to respond to various signals in an extremely rapid and sensitive manner and ultimately improve their fitness and resource economy,[71] as described in *P. fluorescens*[23] and *P. aeruginosa*.[26]

In addition to specific genes subject to catabolite repression control, Hfq and CrcZY have multiple targets, which may confer regulatory plasticity and represent a new layer of hierarchical networks in response to nutritional and environmental cues. As shown in Figure 5, Hfq contributes to optimal root-associated nitrogenase activity via the indirect transcriptional regulation of *nifA* and direct posttranscriptional regulation of

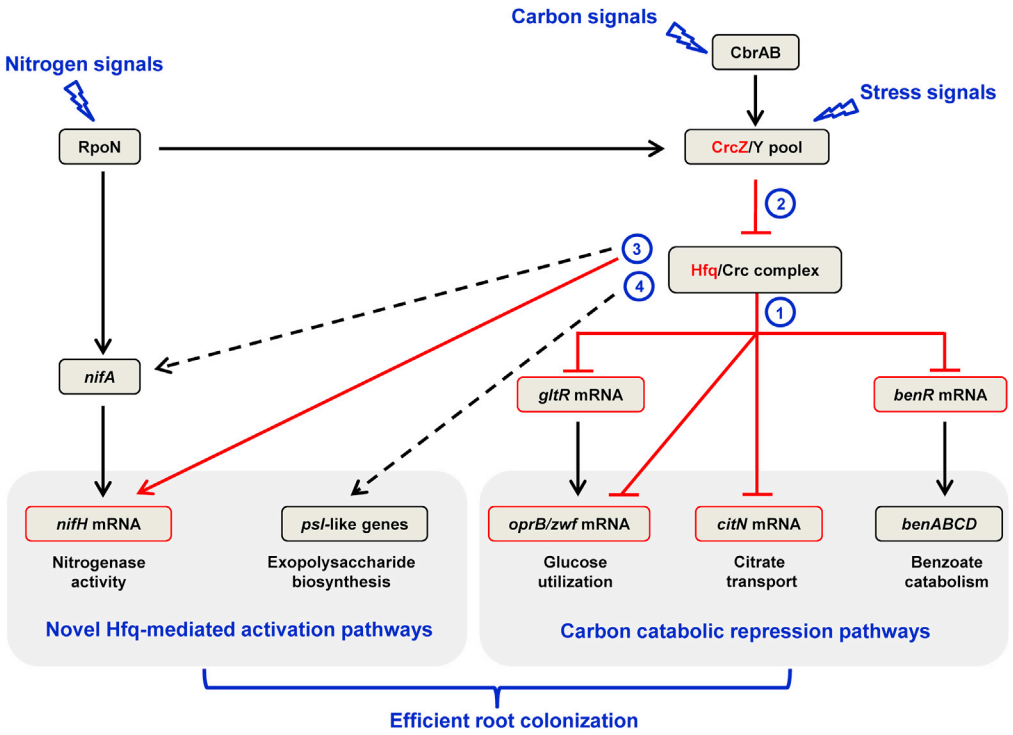

Figure 7. Schematic representation of the regulatory network controlling carbon catabolic repression, nitrogen fixation, and Psl exopolysaccharide biosynthesis in response to environmental signals

A1501 preferentially catabolized the top tier substrates succinate and lactate, followed by relatively less favorable substrate citrate, and ultimately the non-preferred substrates glucose and benzoate. The Hfq/Crc/CrcZY regulatory system orchestrates this preference. ① In the presence of preferred carbon sources, Hfq represses the expression of catabolic targets for non-preferred substrates by binding directly to mRNAs while Crc interacts with Hfq, enhancing the repression exerted by Hfq. ② Non-preferred carbon sources such as glucose and benzoate substantially increase the expression of CrcZ, acting as a key antagonist to Hfq and relieving Hfq-mediated translational repression. In addition, novel Hfq-mediated activation pathways contribute to efficient root colonization. ③ Hfq optimizes root-associated nitrogenase activity by regulating both *nifA* and *nifH* expression at transcriptional and posttranscriptional levels. ④ The intracellular glucose pool is shunted into an as-yet unidentified pathway to produce the Psl exopolysaccharide, which is regulated positively by Hfq at the transcriptional level. Arrows and T-shaped bars indicate positive and negative regulation, respectively. Transcriptional regulation is shown in black, and posttranscriptional regulation is shown in red. Solid lines indicate direct regulation, whereas broken lines indicate indirect regulation through an as yet undetermined mechanism.

nifH. The expression of both *crcZ* and *crcY* is a RpoN-dependent process that is activated by the CbrA/CbrB two component sensor-regulator system (Figures 4F–4I), suggesting a carbon-nitrogen coupling regulation mode. Similar to other *Pseudomonas* strains, A1501 possesses two ncRNAs, CrcZ and CrcY, which can act additively or independently of each other. This functional redundancy may reduce the risk of loss of a critical component of a regulatory pathway. For example, the deletion of either *crcZ* or *crcY* led to a compensatory increase in the levels of the remaining sRNA (Figure 4C). Liu et al. developed a deterministic model and explored the evolutionary conditions for *crcY* and *crcZ* co-existence, proposing that both ncRNAs have different biological functions and confer distinct advantages or disadvantages under specific environmental conditions, e.g. on plant surfaces.[23] Another earlier study showed that *P. putida* growing at low temperature shows increased levels of CrcZ and CrcY, implying their involvement in the cold stress response.[72] We also found that in A1501, the expression of CrcZ and CrcY was associated with environmental stresses (Figure S4). Our data suggest that both ncRNAs might have different functions and consequently different contributions to different stress responses. A similar phenomenon has been described for the ncRNAs RsmY and RsmZ in *P. stutzeri* A1501, both of which have overlapping functions in the regulation of biofilm formation but distinctive roles in the regulation of nitrogen fixation.[64]

Another level of complexity might arise from the positive and negative regulations by Hfq through different modes of action.[71] In one mode, Hfq acts as an RNA matchmaker, promoting base pairing between sRNAs

and their mRNA targets. In a second mode, the chaperone Hfq directly binds the 5′ untranslated region or the coding region of mRNA targets, affecting their translation. Hfq is now recognized as a global regulator of cell physiology, which particularly affects the cell response to several stresses. For example, genetic, phenotypic, and proteomic data reveal wide-ranging effects of Hfq on the basic physiological traits of *P. putida* and *Pseudomonas protegens*.[73,74] Another genome-wide analysis of Hfq-binding RNA targets in *S. meliloti* revealed that major stress response and symbiotic gene networks are extensively subject to Hfq-mediated posttranscriptional regulation.[59] Previously, the *dapB*-based *in vivo* expression system was used to identify the diazotrophic *P. stutzeri* genes induced in the rice rhizosphere, one of which is *hfq*, implying its role in the colonization of rice roots.[44] Although Hfq has been shown to act as a global regulator, there is no information available regarding the mechanism by which this occurs. For example, the nitrogenase complex is composed of the MoFe protein encoded by the *nifD* and *nifK* genes, and the Fe protein encoded by the *nifH* gene. Some root-associated diazotrophs accumulate nitrogenase at levels of as high as 10% of the total soluble proteins within the cells, which would require relatively high levels of *nifHDK* mRNAs than mRNAs encoding other proteins.[75,76] Thus, nitrogen-fixing cells must have a robust capacity to produce *nifHDK* mRNAs at a level sufficient to sustain maximal nitrogenase activity, especially under environmental conditions.[46,77–79] As shown in our previous studies using strain A1501, the NfiR and NfiS, which are induced under nitrogen fixation conditions, optimize nitrogenase activity in a cooperative manner by increasing the stabilities of the *nifD* and *nifK* mRNAs, respectively.[46,77] A reasonable speculation is that *P. stutzeri* A1501 may carry an unidentified ncRNA or employ an unidentified mechanism that specifically targets the *nifH* transcript, as previously described for sRNA154 in *Methanosarcina mazei*.[78] The data presented here indicated that Hfq directly binds the *nifH* mRNA and ultimately enhances nitrogenase activity by increasing the half-life of the *nifH* mRNA, suggesting a novel Hfq-mediated regulatory mechanism underlying the efficient synthesis of the nitrogenase complex. Additionally, the Hfq mutation led to a significant decrease in the expression of *nifA* under nitrogen fixation conditions, as also previously reported.[58,59] This effect is probably indirect, as no Hfq-binding site was identified in either the promoter or coding regions of *nifA*, thus markedly increasing the complexity of the regulatory circuitry.

Numerous investigations have demonstrated that when multiple carbon sources are available, bacteria display the following types of common growth behavior: hierarchical utilization or simultaneous utilization.[1,80] Recent studies suggest that two utilization patterns can coexist during bacterial growth in nutritionally complex environments, allowing cells to allocate cellular resources to achieve optimal growth.[50,81] Our data shown in Figures 7 and S6 provide empirical evidence of a resource allocation strategy that depends on Hfq-mediated opposing regulatory effects as follows: (i) succinate is catabolized as a good carbon and energy source for both growth and nitrogen fixation, while eliciting strong Hfq-mediated repression of glucose utilization that depends on glucokinase encoded by the *glk* gene; (ii) in addition, the intracellular glucose pool is shunted into an as yet unidentified route to produce the Psl exopolysaccharide, which is regulated positively by Hfq and independent of the *glk* gene. Obviously, Hfq-mediated opposing regulatory processes guarantee adequate supply of glucose as a raw material to produce exopolysaccharides, a key factor required for the early stage of both nitrogen-fixing biofilm formation and root colonization.[62,63] We assumed that this strategy on Hfq-mediated opposing regulations may be the result of adaptive evolution within rhizosphere environments. As suggested by Liu et al.,[23] carbon catabolite repression confers a selective disadvantage at the plant surface, a nutritionally complex environment where various carbon sources are present simultaneously but fluctuate in their availability. Our findings further provide a fascinating example of sophisticated regulatory networks underlying carbon substrate utilization, nitrogenase activity, and exopolysaccharide production, which might be a common strategy employed by rhizobacteria to succeed in environments that are nutritionally complex and highly competitive.

Limitations of the study

Metabolically versatile pseudomonads are very competitive, as evidenced by their broad global distributions, for example as highly successful colonizers of the plant rhizosphere; however, the ecological rationale for the carbon catabolite repression strategy employed by rhizobacteria is still an open question.[29] It is interesting to note that the carbon catabolite repression genes also participate in other important biological processes, such as biofilm formation, nutrient uptake, root colonization, and symbiotic nitrogen fixation,[29,59,82] yet the underlying mechanisms are still far from being understood due to their complexities. A key challenge that remains is to develop various tools that will more rapidly and quantitatively characterize the genetic elements and regulatory pathways involved in diazotroph-plant interactions. Progress in this

area will drive the development of new strategies to ensure the compatibility of diazotrophs with host crops and rhizosphere environments, and exploit their potential to the maximum for improving soil fertility and crop growth. Therefore, future studies may provide opportunities to develop synthetic biology approaches that manipulate biofertilizer-producing diazotrophic strains widely used in sustainable agriculture.

STAR★METHODS

Detailed methods are provided in the online version of this paper and include the following:

- KEY RESOURCES TABLE
- RESOURCE AVAILABILITY
  - Lead contact
  - Materials availability
  - Data and code availability
- EXPERIMENTAL MODELS AND SUBJECT DETAILS
  - Bacterial strains and growth conditions
  - Plant materials and growth conditions
- METHOD DETAILS
  - Construction of mutants and complementing strains
  - Construction of translational *lacZ* fusions and β-galactosidase assay
  - Biolog phenotype profiling
  - Rhizosphere colonization and competition assays
  - Strain competition experiment
  - Nitrogenase activity assays
  - Total RNA isolation and quantitative real time RT-PCR (qRT-PCR) analysis
  - 5′ rapid amplification of cDNA ends (5′ RACE) to determine transcriptional start sites
  - Absolute quantification of the RNA copy number using droplet digital PCR (ddPCR)
  - Microscale thermophoresis (MST) analysis
  - Expression and purification of Hfq for MST measurements
  - Expression and purification of Crc and CbrB
  - Expression and purification of RpoN for DNase I footprinting assays
  - DNase I footprinting assays
  - Determination of *nifH* mRNA stability
  - Exopolysaccharide isolation and quantification
  - HPLC analysis of glucose consumption
- QUANTIFICATION AND STATISTICAL ANALYSIS

SUPPLEMENTAL INFORMATION

Supplemental information can be found online at https://doi.org/10.1016/j.isci.2022.105663.

ACKNOWLEDGMENTS

This work was supported by grants from the National Key R&D Program of China (2019YFA0904700 to Y.Y. and 2022YFA0912100 to Y.Z.) and the National Natural Science Foundation of China (31930004 and 32150021 to M.L.). We also appreciate the support from the Institut Pasteur, France.

AUTHORS CONTRIBUTIONS

Y.Z., Y.Y., and M.L. established the research plan and interpreted the results. F.L. and M.L. designed the experiments. F.L. performed the majority of the experiments. Y.Z., Z.Y., and W.L. performed the MST experiments; X.K., S.J., L.S., and W.L. performed the RT-PCR and ddPCR experiments; Y.Z., Y-Y.M., and W.L. performed Biolog phenotyping and analyzed the growth characteristics. X.K., Y.S., Y.Y., S.J., L.S., Y.M., and J.Z. contributed to the construction of the mutants and vectors, protein purification, and the nitrogenase activity and root colonization assays. F.L., Y.Z., L.C., Y.Y., W.L., C.E., and M.L. analyzed data and prepared figures; C.E., Y.Y., and M.L. wrote the article with input from all co-authors.

DECLARATION OF INTERESTS

The authors have no competing interests to declare.

Received: May 27, 2022
Revised: September 8, 2022
Accepted: November 18, 2022
Published: December 22, 2022

REFERENCES

1. Okano, H., Hermsen, R., and Hwa, T. (2021). Hierarchical and simultaneous utilization of carbon substrates: mechanistic insights, physiological roles, and ecological consequences. Curr. Opin. Microbiol. *63*, 172–178.

2. Görke, B., and Stülke, J. (2008). Carbon catabolite repression in bacteria: many ways to make the most out of nutrients. Nat. Rev. Microbiol. *6*, 613–624.

3. Deutscher, J. (2008). The mechanisms of carbon catabolite repression in bacteria. Curr. Opin. Microbiol. *11*, 87–93.

4. Magasanik, B. (1970). Glucose effects: inducer exclusion and repression. In The Lactose Operon, J. Beckwith and D. Zipser, eds. (Cold Spring Harbor Laboratory Press), pp. 189–220.

5. Silby, M.W., Winstanley, C., Godfrey, S.A.C., Levy, S.B., and Jackson, R.W. (2011). *Pseudomonas* genomes: diverse and adaptable. FEMS Microbiol. Rev. *35*, 652–680.

6. Yan, Y., Yang, J., Dou, Y., Chen, M., Ping, S., Peng, J., Lu, W., Zhang, W., Yao, Z., Li, H., et al. (2008). Nitrogen fixation island and rhizosphere competence traits in the genome of root-associated *Pseudomonas stutzeri* A1501. Proc. Natl. Acad. Sci. USA *105*, 7564–7569.

7. Collier, D.N., Hager, P.W., and Phibbs, P.V., Jr. (1996). Catabolite repression control in the pseudomonads. Res. Microbiol. *147*, 551–561.

8. Rojo, F. (2010). Carbon catabolite repression in *Pseudomonas*: optimizing metabolic versatility and interactions with the environment. FEMS Microbiol. Rev. *34*, 658–684.

9. McGill, S.L., Yung, Y., Hunt, K.A., Henson, M.A., Hanley, L., and Carlson, R.P. (2021). *Pseudomonas aeruginosa* reverse diauxie is a multidimensional, optimized, resource utilization strategy. Sci. Rep. *11*, 1457.

10. Hernández-Arranz, S., Sánchez-Hevia, D., Rojo, F., and Moreno, R. (2016). Effect of Crc and Hfq proteins on the transcription, processing, and stability of the *Pseudomonas putida* CrcZ sRNA. RNA *22*, 1902–1917.

11. Sonnleitner, E., Wulf, A., Campagne, S., Pei, X.Y., Wolfinger, M.T., Forlani, G., Prindl, K., Abdou, L., Resch, A., Allain, F.H.T., et al. (2018). Interplay between the catabolite repression control protein Crc, Hfq and RNA in Hfq-dependent translational regulation in *Pseudomonas aeruginosa*. Nucleic Acids Res. *46*, 1470–1485.

12. Malecka, E.M., Bassani, F., Dendooven, T., Sonnleitner, E., Rozner, M., Albanese, T.G., Resch, A., Luisi, B., Woodson, S., and Bläsi, U. (2021). Stabilization of Hfq-mediated translational repression by the co-repressor Crc in *Pseudomonas aeruginosa*. Nucleic Acids Res. *49*, 7075–7087.

13. Moreno, R., Hernández-Arranz, S., La Rosa, R., Yuste, L., Madhushani, A., Shingler, V., and Rojo, F. (2015). The Crc and Hfq proteins of *Pseudomonas putida* cooperate in catabolite repression and formation of ribonucleic acid complexes with specific target motifs. Environ. Microbiol. *17*, 105–118.

14. Pei, X.Y., Dendooven, T., Sonnleitner, E., Chen, S., Bläsi, U., and Luisi, B.F. (2019). Architectural principles for Hfq/Crc-mediated regulation of gene expression. Elife *8*, e43158.

15. Milojevic, T., Grishkovskaya, I., Sonnleitner, E., Djinovic-Carugo, K., and Bläsi, U. (2013). The *Pseudomonas aeruginosa* catabolite repression control protein Crc is devoid of RNA binding activity. PLoS One *8*, e64609.

16. Moreno, R., Martínez-Gomariz, M., Yuste, L., Gil, C., and Rojo, F. (2009a). The *Pseudomonas putida* Crc global regulator controls the hierarchical assimilation of amino acids in a complete medium: evidence from proteomic and genomic analyses. Proteomics *9*, 2910–2928.

17. Hernández-Arranz, S., Moreno, R., and Rojo, F. (2013). The translational repressor Crc controls the *Pseudomonas putida* benzoate and alkane catabolic pathways using a multi-tier regulation strategy. Environ. Microbiol. *15*, 227–241.

18. Moreno, R., Marzi, S., Romby, P., and Rojo, F. (2009b). The Crc global regulator binds to an unpaired A-rich motif at the *Pseudomonas putida alkS* mRNA coding sequence and inhibits translation initiation. Nucleic Acids Res. *37*, 7678–7690.

19. Moreno, R., and Rojo, F. (2008). The target for the *Pseudomonas putida* Crc global regulator in the benzoate degradation pathway is the BenR transcriptional regulator. J. Bacteriol. *190*, 1539–1545.

20. Sonnleitner, E., and Bläsi, U. (2014). Regulation of Hfq by the RNA CrcZ in *Pseudomonas aeruginosa* carbon catabolite repression. PLoS Genet. *10*, e1004440.

21. Sonnleitner, E., Valentini, M., Wenner, N., Haichar, F.e.Z., Haas, D., and Lapouge, K. (2012). Novel targets of the CbrAB/Crc carbon catabolite control system revealed by transcript abundance in *Pseudomonas aeruginosa*. PLoS One *7*, e44637.

22. Sonnleitner, E., Prindl, K., and Bläsi, U. (2017). The *Pseudomonas aeruginosa* CrcZ RNA interferes with Hfq-mediated riboregulation. PLoS One *12*, e0180887.

23. Liu, Y., Gokhale, C.S., Rainey, P.B., and Zhang, X.X. (2017). Unravelling the complexity and redundancy of carbon catabolic repression in *Pseudomonas fluorescens* SBW25. Mol. Microbiol. *105*, 589–605.

24. Browne, P., Barret, M., O'Gara, F., and Morrissey, J.P. (2010). Computational prediction of the Crc regulon identifies genus-wide and species-specific targets of catabolite repression control in *Pseudomonas* bacteria. BMC Microbiol. *10*, 300.

25. Quiroz-Rocha, E., Moreno, R., Hernández-Ortíz, A., Fragoso-Jiménez, J.C., Muriel-Millán, L.F., Guzmán, J., Espín, G., Rojo, F., and Núñez, C. (2017). Glucose uptake in *Azotobacter vinelandii* occurs through a GluP transporter that is under the control of the CbrA/CbrB and Hfq-Crc systems. Sci. Rep. *7*, 858.

26. Sonnleitner, E., Abdou, L., and Haas, D. (2009). Small RNA as global regulator of carbon catabolite repression in *Pseudomonas aeruginosa*. Proc. Natl. Acad. Sci. USA *106*, 21866–21871.

27. Moreno, R., Fonseca, P., and Rojo, F. (2012). Two small RNAs, CrcY and CrcZ, act in concert to sequester the Crc global regulator in *Pseudomonas putida*, modulating catabolite repression. Mol. Microbiol. *83*, 24–40.

28. Filiatrault, M.J., Stodghill, P.V., Wilson, J., Butcher, B.G., Chen, H., Myers, C.R., and Cartinhour, S.W. (2013). CrcZ and CrcX regulate carbon source utilization in *Pseudomonas syringae* pathovar tomato strain DC3000. RNA Biol. *10*, 245–255.

29. Franzino, T., Boubakri, H., Cernava, T., Abrouk, D., Achouak, W., Reverchon, S., Nasser, W., and Haichar, F.E.Z. (2022). Implications of carbon catabolite repression for plant-microbe interactions. Plant Commun. *3*, 100272.

30. Chakravarthy, S., Butcher, B.G., Liu, Y., D'Amico, K., Coster, M., and Filiatrault, M.J. (2017). Virulence of *Pseudomonas syringae pv. tomato* DC3000 is influenced by the catabolite repression control protein Crc. Mol. Plant Microbe Interact. *30*, 283–294.

31. Bharwad, K., Ghoghari, N., and Rajkumar, S. (2021). Crc regulates succinate-mediated repression of mineral phosphate solubilization in *Acinetobacter* sp. SK2 by modulating membrane glucose dehydrogenase. Front. Microbiol. *12*, 641119.

32. Patel, D.K., Murawala, P., Archana, G., and Kumar, G.N. (2011). Repression of mineral phosphate solubilizing phenotype in the presence of weak organic acids in plant growth promoting fluorescent pseudomonads. Bioresour. Technol. *102*, 3055–3061.

33. Diab, F., Bernard, T., Bazire, A., Haras, D., Blanco, C., and Jebbar, M. (2006). Succinate-mediated catabolite repression control on the production of glycine betaine catabolic enzymes in *Pseudomonas aeruginosa* PAO1 under low and elevated salinities. Microbiology *152*, 1395–1406.

34. Rajput, M.S., Naresh Kumar, G., and Rajkumar, S. (2013). Repression of oxalic acid-mediated mineral phosphate solubilization in rhizospheric isolates of *Klebsiella pneumoniae* by succinate. Arch. Microbiol. *195*, 81–88.

35. Joshi, E., Iyer, B., and Rajkumar, S. (2019). Glucose and arabinose dependent mineral phosphate solubilization and its succinate-mediated catabolite repression in *Rhizobium* sp. RM and RS. J. Biosci. Bioeng. *128*, 551–557.

36. Bloch, S.E., Clark, R., Gottlieb, S.S., Wood, L.K., Shah, N., Mak, S.M., Lorigan, J.G., Johnson, J., Davis-Richardson, A.G., Williams, L., et al. (2020). Biological nitrogen fixation in maize: optimizing nitrogenase expression in a root-associated diazotroph. J. Exp. Bot. *71*, 4591–4603.

37. Bürgmann, H., Meier, S., Bunge, M., Widmer, F., and Zeyer, J. (2005). Effects of model root exudates on structure and activity of a soil diazotroph community. Environ. Microbiol. *7*, 1711–1724.

38. Parys, K., Colaianni, N.R., Lee, H.S., Hohmann, U., Edelbacher, N., Trgovcevic, A., Blahovska, Z., Lee, D., Mechtler, A., Muhari-Portik, Z., et al. (2021). Signatures of antagonistic pleiotropy in a bacterial flagellin epitope. Cell Host Microbe *29*, 620–634.e9.

39. Jain, R., and Kazmierczak, B.I. (2019). Should I stay or should I go? *Pseudomonas* just can't decide. Cell Host Microbe *25*, 5–7.

40. Mavrodi, O.V., McWilliams, J.R., Peter, J.O., Berim, A., Hassan, K.A., Elbourne, L.D.H., LeTourneau, M.K., Gang, D.R., Paulsen, I.T., Weller, D.M., et al. (2021). Root exudates alter the expression of diverse metabolic, transport, regulatory, and stress response genes in rhizosphere *Pseudomonas*. Front. Microbiol. *12*, 651282.

41. Loper, J.E., Hassan, K.A., Mavrodi, D.V., Davis, E.W., 2nd, Lim, C.K., Shaffer, B.T., Elbourne, L.D.H., Stockwell, V.O., Hartney, S.L., Breakwell, K., et al. (2012). Comparative genomics of plant-associated *Pseudomonas* spp.: insights into diversity and inheritance of traits involved in multitrophic interactions. PLoS Genet. *8*, e1002784.

42. Lugtenberg, B.J., Dekkers, L., and Bloemberg, G.V. (2001). Molecular determinants of rhizosphere colonization by *Pseudomonas*. Annu. Rev. Phytopathol. *39*, 461–490.

43. You, C., and Zhou, F. (1989). Non-nodular endorhizospheric nitrogen fixation in wetland rice. Can. J. Microbiol. *35*, 403–408.

44. Rediers, H., Bonnecarrère, V., Rainey, P.B., Hamonts, K., Vanderleyden, J., and De Mot, R. (2003). Development and application of a *dapB*-based in vivo expression technology system to study colonization of rice by the endophytic nitrogen-fixing bacterium *Pseudomonas stutzeri* A15. Appl. Environ. Microbiol. *69*, 6864–6874.

45. Lin, M., Yan, Y., Lu, W., Zhan, Y., Zhang, Y., and Elmerich, C. (2015). Regulatory coupling of nitrogen and carbon metabolisms in nitrogen-fixing *Pseudomonas stutzeri* A1501. In Biological Nitrogen Fixation, F.J. de Bruijn, ed. (Wiley Blackwell), pp. 109–119.

46. Zhan, Y., Yan, Y., Deng, Z., Chen, M., Lu, W., Lu, C., Shang, L., Yang, Z., Zhang, W., Wang, W., et al. (2016). The novel regulatory ncRNA, NfiS, optimizes nitrogen fixation via base pairing with the nitrogenase gene *nifK* mRNA in *Pseudomonas stutzeri* A1501. Proc. Natl. Acad. Sci. USA *113*, E4348–E4356.

47. Drepper, T., Raabe, K., Giaourakis, D., Gendrullis, M., Masepohl, B., and Klipp, W. (2002). The Hfq-like protein NrfA of the phototrophic purple bacterium *Rhodobacter capsulatus* controls nitrogen fixation via regulation of *nifA* and *anfA* expression. FEMS Microbiol. Lett. *215*, 221–227.

48. Li, D., Yan, Y., Ping, S., Chen, M., Zhang, W., Li, L., Lin, W., Geng, L., Liu, W., Lu, W., et al. (2010). Genome-wide investigation and functional characterization of the beta-ketoadipate pathway in the nitrogen-fixing and root-associated bacterium *Pseudomonas stutzeri* A1501. BMC Microbiol. *10*, 36.

49. Karishma, M., Trivedi, V.D., Choudhary, A., Mhatre, A., Kambli, P., Desai, J., and Phale, P.S. (2015). Analysis of preference for carbon source utilization among three strains of aromatic compounds degrading *Pseudomonas*. FEMS Microbiol. Lett. *362*, fnv139.

50. Wang, X., Xia, K., Yang, X., and Tang, C. (2019). Growth strategy of microbes on mixed carbon sources. Nat. Commun. *10*, 1279.

51. Conway, T. (1992). The Entner-Doudoroff pathway: history, physiology and molecular biology. FEMS Microbiol. Rev. *9*, 1–27.

52. Daddaoua, A., Molina-Santiago, C., de la Torre, J., Krell, T., and Ramos, J.L. (2014). GtrS and GltR form a two-component system: the central role of 2-ketogluconate in the expression of exotoxin A and glucose catabolic enzymes in *Pseudomonas aeruginosa*. Nucleic Acids Res. *42*, 7654–7663.

53. Valentini, M., García-Mauriño, S.M., Pérez-Martínez, I., Santero, E., Canosa, I., and Lapouge, K. (2014). Hierarchical management of carbon sources is regulated similarly by the CbrA/B systems in *Pseudomonas aeruginosa* and *Pseudomonas putida*. Microbiology *160*, 2243–2252.

54. La Rosa, R., Nogales, J., and Rojo, F. (2015). The Crc/CrcZ-CrcY global regulatory system helps the integration of gluconeogenic and glycolytic metabolism in *Pseudomonas putida*. Environ. Microbiol. *17*, 3362–3378.

55. García-Mauriño, S.M., Pérez-Martínez, I., Amador, C.I., Canosa, I., and Santero, E. (2013). Transcriptional activation of the CrcZ and CrcY regulatory RNAs by the CbrB response regulator in *Pseudomonas putida*. Mol. Microbiol. *89*, 189–205.

56. Wahab, A.M.A., and Wareing, P.F. (1980). Nitrogenase activity associated with the rhizosphere of *Ammophila arenaria* L. and effect of inoculation of seedings with *Azotobacter*. New Phytol. *84*, 711–721.

57. Elbeltagy, A., Nishioka, K., Sato, T., Suzuki, H., Ye, B., Hamada, T., Isawa, T., Mitsui, H., and Minamisawa, K. (2001). Endophytic colonization and in planta nitrogen fixation by a *Herbaspirillum* sp. isolated from wild rice species. Appl. Environ. Microbiol. *67*, 5285–5293.

58. Kaminski, P.A., Desnoues, N., and Elmerich, C. (1994). The expression of *nifA* in *Azorhizobium caulinodans* requires a gene product homologous to *Escherichia coli* HF-I, an RNA-binding protein involved in the replication of phage Q beta RNA. Proc. Natl. Acad. Sci. USA *91*, 4663–4667.

59. Torres-Quesada, O., Reinkensmeier, J., Schlüter, J.P., Robledo, M., Peregrina, A., Giegerich, R., Toro, N., Becker, A., and Jiménez-Zurdo, J.I. (2014). Genome-wide profiling of Hfq-binding RNAs uncovers extensive post-transcriptional rewiring of major stress response and symbiotic regulons in *Sinorhizobium meliloti*. RNA Biol. *11*, 563–579.

60. Heredia-Ponce, Z., de Vicente, A., Cazorla, F.M., and Gutiérrez-Barranquero, J.A. (2021). Beyond the wall: exopolysaccharides in the biofilm lifestyle of pathogenic and beneficial plant-associated *Pseudomonas*. Microorganisms *9*, 445.

61. Kirisits, M.J., Prost, L., Starkey, M., and Parsek, M.R. (2005). Characterization of colony morphology variants isolated from *Pseudomonas aeruginosa* biofilms. Appl. Environ. Microbiol. *71*, 4809–4821.

62. Meneses, C.H.S.G., Rouws, L.F.M., Simoes-Araujo, J.L., Vidal, M.S., and Baldani, J.I. (2011). Exopolysaccharide production is required for biofilm formation and plant colonization by the nitrogen-fixing endophyte *Gluconacetobacter diazotrophicus*. Mol. Plant Microbe Interact. *24*, 1448–1458.

63. Byrd, M.S., Sadovskaya, I., Vinogradov, E., Lu, H., Sprinkle, A.B., Richardson, S.H., Ma, L., Ralston, B., Parsek, M.R., Anderson, E.M., et al. (2009). Genetic and biochemical analyses of the *Pseudomonas aeruginosa* Psl exopolysaccharide reveal overlapping roles for polysaccharide synthesis enzymes in Psl and LPS production. Mol. Microbiol. *73*, 622–638.

64. Shang, L., Yan, Y., Zhan, Y., Ke, X., Shao, Y., Liu, Y., Yang, H., Wang, S., Dai, S., Lu, J., et al.

(2021). A regulatory network involving Rpo, Gac and Rsm for nitrogen-fixing biofilm formation by *Pseudomonas stutzeri*. NPJ Biofilms Microbiomes *7*, 54.

65. Daddaoua, A., Krell, T., and Ramos, J.L. (2009). Regulation of glucose metabolism in *Pseudomonas*: the phosphorylative branch and entner-doudoroff enzymes are regulated by a repressor containing a sugar isomerase domain. J. Biol. Chem. *284*, 21360–21368.

66. Pérez-Pantoja, D., Leiva-Novoa, P., Donoso, R.A., Little, C., Godoy, M., Pieper, D.H., and González, B. (2015). Hierarchy of carbon source utilization in soil bacteria: hegemonic preference for benzoate in complex aromatic compound mixtures degraded by *Cupriavidus pinatubonensis* strain JMP134. Appl. Environ. Microbiol. *81*, 3914–3924.

67. Cheng, Y.T., Zhang, L., and He, S.Y. (2019). Plant-microbe interactions facing environmental challenge. Cell Host Microbe *26*, 183–192.

68. Fröschel, C., Komorek, J., Attard, A., Marsell, A., Lopez-Arboleda, W.A., Le Berre, J., Wolf, E., Geldner, N., Waller, F., Korte, A., et al. (2021). Plant roots employ cell-layer-specific programs to respond to pathogenic and beneficial microbes. Cell Host Microbe *29*, 299–310.e7.

69. Vives-Peris, V., de Ollas, C., Gómez-Cadenas, A., and Pérez-Clemente, R.M. (2020). Root exudates: from plant to rhizosphere and beyond. Plant Cell Rep. *39*, 3–17.

70. Martínez-Valenzuela, M., Guzmán, J., Moreno, S., Ahumada-Manuel, C.L., Espín, G., and Núñez, C. (2018). Expression of the sRNAs CrcZ and CrcY modulate the strength of carbon catabolite repression under diazotrophic or non-diazotrophic growing conditions in *Azotobacter vinelandii*. PLoS One *13*, e0208975.

71. Grenga, L., Little, R.H., and Malone, J.G. (2017). Quick change: post-transcriptional regulation in *Pseudomonas*. FEMS Microbiol. Lett. *364*, fnx125.

72. Fonseca, P., Moreno, R., and Rojo, F. (2013). *Pseudomonas putida* growing at low temperature shows increased levels of CrcZ and CrcY sRNAs, leading to reduced Crc-dependent catabolite repression. Environ. Microbiol. *15*, 24–35.

73. Arce-Rodríguez, A., Calles, B., Nikel, P.I., and de Lorenzo, V. (2016). The RNA chaperone Hfq enables the environmental stress tolerance super-phenotype of *Pseudomonas putida*. Environ. Microbiol. *18*, 3309–3326.

74. Wang, Z., Huang, X., Jan, M., Kong, D., Pan, J., and Zhang, X. (2021). The global regulator Hfq exhibits far more extensive and intensive regulation than Crc in *Pseudomonas protegens* H78. Mol. Plant Pathol. *22*, 921–938.

75. Yan, Y., Ping, S., Peng, J., Han, Y., Li, L., Yang, J., Dou, Y., Li, Y., Fan, H., Fan, Y., et al. (2010). Global transcriptional analysis of nitrogen fixation and ammonium repression in root-associated *Pseudomonas stutzeri* A1501. BMC Genom. *11*, 11.

76. Dingler, C., Kuhla, J., Wassink, H., and Oelze, J. (1988). Levels and activities of nitrogenase proteins in *Azotobacter vinelandii* grown at different dissolved oxygen concentrations. J. Bacteriol. *170*, 2148–2152.

77. Zhan, Y., Deng, Z., Yan, Y., Zhang, H., Lu, C., Yang, Z., Shang, L., Huang, Y., Lv, F., Liu, Y., et al. (2019). NfiR, a new regulatory noncoding RNA (ncRNA), is required in concert with the NfiS ncRNA for optimal expression of nitrogenase genes in *Pseudomonas stutzeri* A1501. Appl. Environ. Microbiol. *85*. e00762007622-19.

78. Prasse, D., Förstner, K.U., Jäger, D., Backofen, R., and Schmitz, R.A. (2017). sRNA154 a newly identified regulator of nitrogen fixation in *Methanosarcina mazei* strain Go1. RNA Biol. *14*, 1544–1558.

79. Silveira, R., Mello, T.R.B., Sartori, M.R.S., Alves, G.S.C., Fonseca, F.C.A., Vizzotto, C.S., Krüger, R.H., and Bustamante, M. (2021). Seasonal and long-term effects of nutrient additions and liming on the *nifH* gene in cerrado soils under native vegetation. iScience *24*, 102349.

80. Okano, H., Hermsen, R., Kochanowski, K., and Hwa, T. (2020). Regulation underlying hierarchical and simultaneous utilization of carbon substrates by flux sensors in *Escherichia coli*. Nat. Microbiol. *5*, 206–215.

81. Perrin, E., Ghini, V., Giovannini, M., Di Patti, F., Cardazzo, B., Carraro, L., Fagorzi, C., Turano, P., Fani, R., and Fondi, M. (2020). Diauxie and co-utilization of carbon sources can coexist during bacterial growth in nutritionally complex environments. Nat. Commun. *11*, 3135.

82. O'Gara, F., Birkenhead, K., Boesten, B., and Fitzmaurice, A.M. (1989). Carbon metabolism and catabolite repression in *Rhizobium* spp. FEMS Microbiol. Rev. *5*, 93–101.

83. Figurski, D.H., and Helinski, D.R. (1979). Replication of an origin-containing derivative of plasmid RK2 dependent on a plasmid function provided in trans. Proc. Natl. Acad. Sci. USA *76*, 1648–1652.

84. Schäfer, A., Tauch, A., Jäger, W., Kalinowski, J., Thierbach, G., and Pühler, A. (1994). Small mobilizable multi-purpose cloning vectors derived from the *Escherichia coli* plasmids pK18 and pK19: selection of defined deletions in the chromosome of *Corynebacterium glutamicum*. Gene *145*, 69–73.

85. Choi, K.H., Gaynor, J.B., White, K.G., Lopez, C., Bosio, C.M., Karkhoff-Schweizer, R.R., and Schweizer, H.P. (2005). A Tn7-based broad-range bacterial cloning and expression system. Nat. Methods *2*, 443–448.

86. Staskawicz, B., Dahlbeck, D., Keen, N., and Napoli, C. (1987). Molecular characterization of cloned avirulence genes from race 0 and race 1 of *Pseudomonas syringae pv. glycinea*. J. Bacteriol. *169*, 5789–5794.

87. Liu, Y., Rainey, P.B., and Zhang, X.X. (2014). Mini-Tn7 vectors for studying post-transcriptional gene expression in *Pseudomonas*. J. Microbiol. Methods *107*, 182–185.

88. Desnoues, N., Lin, M., Guo, X., Ma, L., Carreño-Lopez, R., and Elmerich, C. (2003). Nitrogen fixation genetics and regulation in a *Pseudomonas stutzeri* strain associated with rice. Microbiology *149*, 2251–2262.

89. Shevchuk, N.A., Bryksin, A.V., Nusinovich, Y.A., Cabello, F.C., Sutherland, M., and Ladisch, S. (2004). Construction of long DNA molecules using long PCR-based fusion of several fragments simultaneously. Nucleic Acids Res. *32*, e19.

90. Durand, S., Callan-Sidat, A., McKeown, J., Li, S., Kostova, G., Hernandez-Fernaud, J.R., Alam, M.T., Millard, A., Allouche, D., Constantinidou, C., et al. (2021). Identification of an RNA sponge that controls the RoxS riboregulator of central metabolism in *Bacillus subtilis*. Nucleic Acids Res. *49*, 6399–6419.

91. Lippok, S., Seidel, S.A.I., Duhr, S., Uhland, K., Holthoff, H.P., Jenne, D., and Braun, D. (2012). Direct detection of antibody concentration and affinity in human serum using microscale thermophoresis. Anal. Chem. *84*, 3523–3530.

92. Wang, Y., Cen, X.F., Zhao, G.P., and Wang, J. (2012). Characterization of a new GlnR binding box in the promoter of *amtB* in *Streptomyces coelicolor* inferred a PhoP/GlnR competitive binding mechanism for transcriptional regulation of *amtB*. J. Bacteriol. *194*, 5237–5244.

93. Paulo, E.M., Boffo, E.F., Branco, A., Valente, A.M.M.P., Melo, I.S., Ferreira, A.G., Roque, M.R.A., and Assis, S.A. (2012). Production, extraction and characterization of exopolysaccharides produced by the native *Leuconostoc pseudomesenteroides* R2 strain. An. Acad. Bras. Cienc. *84*, 495–508.

94. Nielsen, S.S. (2010). Phenol-sulfuric acid method for total carbohydrates. In Food Analysis Laboratory Manual. Food Science Texts Series, S.S. Nielsen, ed. (Springer).

95. Guan, Y.G., Yu, P., Yu, S.J., Xu, X.B., and Wu, X.L. (2012). Short communication: simultaneous analysis of reducing sugars and 5-hydroxymethyl-2-furaldehyde at a low concentration by high performance anion exchange chromatography with electrochemical detector, compared with HPLC with refractive index detector. J. Dairy Sci. *95*, 6379–6383.

STAR★METHODS

KEY RESOURCES TABLE

REAGENT or RESOURCE	SOURCE	IDENTIFIER
Bacterial strains		
Pseudomonas stutzeri A1501	CGMCC 0351	N/A
Pseudomonas stutzeri A1501 *Δhfq*	This study	N/A
Pseudomonas stutzeri A1501 *Δhfq* (p*Lhfq*)	This study	N/A
Pseudomonas stutzeri A1501 *Δcrc*	This study	N/A
Pseudomonas stutzeri A1501 *Δcrc* (p*Lcrc*)	This study	N/A
Pseudomonas stutzeri A1501 *Δhfqcrc*	This study	N/A
Pseudomonas stutzeri A1501 *Δhfqcrc* (p*Lhfq*)	This study	N/A
Pseudomonas stutzeri A1501 *Δhfqcrc* (p*Lcrc*)	This study	N/A
Pseudomonas stutzeri A1501 *ΔcbrA*	This study	N/A
Pseudomonas stutzeri A1501 *ΔcbrA* (p*LcbrA*)	This study	N/A
Pseudomonas stutzeri A1501 *ΔcbrB*	This study	N/A
Pseudomonas stutzeri A1501 *ΔcbrB* (p*LcbrB*)	This study	N/A
Pseudomonas stutzeri A1501 *ΔrpoN*	Shang et al.[64]	N/A
Pseudomonas stutzeri A1501 *ΔrpoN* (p*LrpoN*)	Shang et al.[64]	N/A
Pseudomonas stutzeri A1501 *ΔcrcZ*	This study	N/A
Pseudomonas stutzeri A1501 *ΔcrcZ* (p*LcrcZ*)	This study	N/A
Pseudomonas stutzeri A1501 *ΔcrcY*	This study	N/A
Pseudomonas stutzeri A1501 *ΔcrcY* (p*LcrcY*)	This study	N/A
Pseudomonas stutzeri A1501 *ΔcrcYcrcZ*	This study	N/A
Pseudomonas stutzeri A1501 *ΔcrcYcrcZ* (p*LcrcZ*)	This study	N/A
Pseudomonas stutzeri A1501 *ΔcrcYcrcZ* (p*LcrcY*)	This study	N/A
Pseudomonas stutzeri A1501 *ΔglK*	This study	N/A
Pseudomonas stutzeri A1501 *ΔpslA*	Shang et al.[64]	N/A
Pseudomonas stutzeri A1501 *edd::lacZ*	This study	N/A
Pseudomonas stutzeri A1501 *gltR::lacZ*	This study	N/A
Escherichia coli DH5a	NEB	Cat# C2987H
Escherichia coli BL21	NEB	Cat# C2527H
Chemicals, peptides, and recombinant proteins		
D-Glucose	Sigma-Aldrich	Cat# G8270
Succinic acid	Thermo Scientific	Cat# A12084.36
Sodium lactate	Thermo Scientific	Cat# L14500.06
Sodium benzoate	Thermo Scientific	Cat# 447802500
Sodium citrate	Sigma-Aldrich	Cat# PHR1416
Potassium phosphate monobasic	Aladdin	Cat# P104078
Potassium hydrogen phosphate	Aladdin	Cat# P112219
Sodium chloride	Aladdin	Cat# C111538
Magnesium sulfate	Aladdin	Cat# M110771
Manganese sulfate monohydrate	Aladdin	Cat# M111712
Iron (III) sulfate hydrate	Aladdin	Cat# F112483

(*Continued on next page*)

Continued

REAGENT or RESOURCE	SOURCE	IDENTIFIER
Sodium molybdate dihydrate	Aladdin	Cat# S104871
DMSO	Invitrogen	Cat# D12345
EDTA	Aladdin	Cat# E116429
EDTA-Ca	Sigma-Aldrich	Cat# 340073-100G
PBS	MP Biomedicals	Cat# PBS10X02
Tris-HCl	Solarbio	Cat# T8230
Yeast Extract Powder	Oxoid	Cat# LP0021B
Tryptone	Oxoid	Cat# LP0042B
Sulfuric acid	Sigma-Aldrich	Cat# 258105
Ethanol	Thermo Scientific	Cat# 611050040
Water-Saturated Phenol	Invitrogen	Cat# AM9712
Gentamicin	Sigma-Aldrich	Cat# G1264-5G
Hygromycin B	Sigma-Aldrich	Cat# SBR00039
Spectinomycin	Sigma-Aldrich	Cat# S9007-5G-9
Kanamycin	Sigma-Aldrich	Cat# E004000-5G
Ampicillin	Sigma-Aldrich	Cat# A5354
Tetracycline hydrochloride	Thermo Scientific	Cat# 233100025
HEPES buffer	GIBCO	Cat# 15630080
Trimethylamine	Sigma-Aldrich	Cat# 471283
β-Mercaptoethanol	Sigma-Aldrich	Cat# 444203
DTT	Thermo Scientific	Cat# R0861
RNAlater solution	Invitrogen	Cat# AM7020
Xba I	NEB	Cat# R0145S
Sph I-HF	NEB	Cat# R3182S
Nhe I-HF	NEB	Cat# R3131S
*Eco*R I-HF	NEB	Cat# R3101S
*Bam*H I -HF	NEB	Cat# R3136S
Hind III-HF	NEB	Cat# R3104S
Nde I	NEB	Cat# R0111S
Spe I-HF	NEB	Cat# R3133S
Xho I	NEB	Cat# R0146S
Nco I-HF	NEB	Cat# R3193S
4-Methylumbelliferyl-b-D-galactoside	Sigma-Aldrich	Cat# 4368814
7-Hydroxy-4-methylcoumarin	Sigma-Aldrich	Cat# 128724
DNase I	Promega	Cat# M6101
Biolog GENIII MicroPlate	BioLog	Cat# 1030
Strep-Tactin column	IBA LifeSciences	Cat# 12-4013-001
Chitin Beads	NEB	Cat# S6651V
Buffer W	IBA LifeSciences	Cat# 2-1003-100
REAGENT or RESOURCE	SOURCE	IDENTIFIER
Buffer BXT	IBA LifeSciences	Cat# 2-1042-025
Sodium hypochlorite	Thermo Scientific	Cat# 219255000
RNAClean XP	Beckman coulter	Cat# A66514
Critical commercial assays		
ClonExpress II One Step Cloning Kit	Vazyme	Cat# C112-01

(*Continued on next page*)

Continued

REAGENT or RESOURCE	SOURCE	IDENTIFIER
TIANamp Bacteria DNA Kit	TIANGEN	Cat# DP302
M5 HiPer Multi-color Plasmid Miniprep Kit	Mei5bio	Cat# MF031-plus-04
CloneJET PCR Cloning Kit	Thermo Scientific	Cat# K1232
High-Capacity cDNA Reverse Transcription Kit	ABI	Cat# 4368814
T7 High Yield RNA Transcription Kit	Vazyme	Cat# TR101-01
Quick Start Bradford Protein Assay Kit	Bio-Rad	Cat# 5000201
InnuPREP RNA Mini Kit	Analytik Jena	Cat# 10755-390
PowerUp SYBR Green PCR Master Mix	ABI	Cat# 01118369
5′ RACE System for Rapid Amplification of cDNA Ends	Invitrogen	Cat# 18374-058
2 × EvaGreen ddPCR SuperMix	Bio-Rad	Cat# 186-4034
Ni-NTA Fast Start Kit	Qiagen	Cat# 30600
Protein labeling Kit RED-NHS	NanoTemper	Cat# L001
Experimental models: Organisms/strains		
Zhonghua 11 (*Oryza sativa* L. subsp. Japonica)	Chinese Academy of Agricultural Sciences	N/A
Oligonucleotides (Primers used in this study, see Table S4)		
Recombinant DNA		
pRK2013	Lab collection Figurski and Helinski,[83]	N/A
pK18*mob*	Lab collection Schäfer et al.[84]	N/A
pK18*mobsacB*	Lab collection Schäfer et al.[84]	N/A
pUX-BF13	Lab collection Choi et al.[85]	N/A
pMD18-T	TaKaRa	Cat# 6011
pLAFR3	Lab collection Staskawicz et al.[86]	N/A
pXY2	Lab collection Liu et al.[87]	N/A
pET30a	Novagen	Cat# 69909
pET28a	Novagen	Cat# 69864
pTWIN1	NEB	Cat # N6951S
pK18*mob-glk*	This study	N/A
pKatCA75	Lab collection	N/A
pKatHPH4	Lab collection	N/A
pKatAAD2	Lab collection	N/A
pK18*mobsacB-hfq*	This study	N/A
pK18*mobsacB-crc*	This study	N/A
pK18*mobsacB-crcZ*	This study	N/A
pK18*mobsacB-crcY*	This study	N/A
pK18*mobsacB-cbrA*	This study	N/A
pK18*mobsacB-cbrB*	This study	N/A
pXY2-P*edd*	This study	N/A
pXY2-P*gltR*	This study	N/A
p*Lhfq*	This study	N/A
p*LcbrA*	This study	N/A
p*LcrcY*	This study	N/A

(*Continued on next page*)

Continued

REAGENT or RESOURCE	SOURCE	IDENTIFIER
pL*crcZ*	This study	N/A
pL*crc*	This study	N/A
pET30a-*hfq*	This study	N/A
pTW-*crc*	This study	N/A
pET28a-*rpoN*	This study	N/A
pTW-*cbrB*	This study	N/A
Software and algorithms		
MEGA 6	N/A	https://www.megasoftware.net
Primer Premier 5.0	N/A	http://www.premierbiosoft.com/primerdesign/
GraphPad Prism 9.0	N/A	https://www.graphpad.com/
SnapGene 3.2.1	N/A	https://www.snapgene.com/

RESOURCE AVAILABILITY

Lead contact

Further information and requests for resources and reagents should be directed to and will be fulfilled by the lead contact, Min Lin (linmin@caas.cn).

Materials availability

This study did not generate new unique reagents.

Data and code availability

- All data reported in this paper will be shared by the lead contact upon request.
- This paper does not report original code.
- Any additional information required to reanalyze the data reported in this paper is available from the lead contact upon request.

EXPERIMENTAL MODELS AND SUBJECT DETAILS

Bacterial strains and growth conditions

P. stutzeri A1501 and its derivatives were grown on LB medium or minimal medium K (containing 0.4 g L^{-1} KH_2PO_4, 0.1 g L^{-1} K_2HPO_4, 0.1 g L^{-1} NaCl, 0.2 g L^{-1} $MgSO_4 \cdot 7H_2O$, 0.01 g L^{-1} $MnSO_4 \cdot H_2O$, 0.01 g L^{-1} $Fe_2(SO_4)_3 \cdot H_2O$, and 0.01 g L^{-1} $Na_2MoO_4 \cdot H_2O$, pH 6.8) supplemented with the indicated carbon and nitrogen sources.[88] Unless stated otherwise, growth experiments were conducted using minimal medium K containing NH_4^+ (6.0 mM) and succinate (20 mM) as sole nitrogen and carbon sources with agitation at 200 rpm at 30°C. For diauxic measurements, minimal medium K was supplemented with an excess concentration of glucose (20 mM) plus a preferred carbon source at a concentration (4 mM) insufficient to support full growth, on which A1501 grow in a diauxic manner. If needed, *E. coli* and A1501 were grown in the presence of 100 μg mL^{-1} ampicillin (Amp), 10 μg mL^{-1} tetracycline (Tc), or chloramphenicol (Cm), 50 μg mL^{-1} spectinomycin (Spc), 50 μg mL^{-1} gentamicin sulfate (Gm), 50 μg mL^{-1} kanamycin (Km) and 50 μg mL^{-1} hygromycin (Hyg). The absorbance (OD_{600}) was measured with a U-3010 (Hitachi) spectrophotometer.

Plant materials and growth conditions

The rice seeds (zhonghua11 from a rice-breeding program at the Chinese Academy of Agricultural Sciences) were surface sterilized by a 2 min soak in 75% (v/v) ethanol, followed by 10 min in sodium hypochlorite solution (10% active chlorine). The seeds were rinsed five times (5 min each time) with sterile distilled water and germinated on humid sterile filter paper at 30°C. Three-day-old seedlings were transferred to the beaker containing sterilized MS medium (1.65 g L^{-1} NH_4NO_3, 0.44 g L^{-1} $CaCl_2 \cdot 2H_2O$, 0.37 g L^{-1} $MgSO_4 \cdot 7H_2O$, 0.17 mg L^{-1} KH_2PO_4, 1.9 g L^{-1} KNO_3, 6.2 mg L^{-1} H_3BO_3, 0.025 mg L^{-1} $CoCl_2 \cdot 6H_2O$, 27.8 mg L^{-1} $FeSO_4 \cdot 7H_2O$, 22.3 mg L^{-1} $MnSO_4 \cdot 4H_2O$, 0.83 mg L^{-1} KI, 0.25 mg L^{-1} $Na_2MoO_4 \cdot 2H_2O$,

8.6 mg L^{-1} $ZnSO_4 \cdot 7H_2O$, 36.7 mg L^{-1} FeNaEDTA, and 0.025 mg L^{-1} $CuSO_4 \cdot 5H_2O$, pH 6.0), and then incubated in a MGC-350HP-2L plant growth cabinet (Shanghai Bluepard Instruments Co.) under a light-dark cycle (16 h of 3000 Lux light at 28°C and 8 h of dark at 25°C, 60% relative humidity) for 12 days until further analysis.

METHOD DETAILS

Construction of mutants and complementing strains

To generate mutant strains, an in-frame gene deletion was introduced into the *Pseudomonas stutzeri* chromosome by homologous recombination,[64] as shown in Figure S7. Appropriate oligonucleotide primers (see Table S4) were designed to generate amplicons that were cloned into the pK18mob vector,[84] and the resulting plasmids were introduced into A1501 by triparental mating using pRK2013[83] as the helper plasmid, and chromosomally integrated upon first cross-over selection for Km and corresponding antibiotic resistances. Excision of the vector in the second cross-over was obtained through enrichment of Km-sensitive cells on 10% (wt/vol) sucrose and corresponding antibiotic-supplemented plates. The Cm resistance gene was amplified by PCR from pKatCA75 for the construction of Δ*crc*, Δ*cbrA*, and Δ*cbrB*. The Hyg resistance gene was amplified from pKatHPH4 for the construction of Δ*hfq*, Δ*crcZ,* and Δ*crcY*. The Spec resistance gene was amplified from pKatAAD2 for the construction of Δ*hfq*, Δ*crcZ,* and Δ*crcY*. Correct recombination was confirmed by PCR followed by nucleotide sequencing of the amplicons obtained. After recombination in the host genome, genes located downstream of the insertion (when part of the same operon) were transcribed from the promoter of the resistance gene, and the expression levels of downstream genes in WT and mutant strains under normal growth conditions were compared using qRT-PCR.

The complemented strains were constructed using the broad host plasmid pLAFR3. A DNA fragment containing a WT gene with its promoter and terminator was amplified from genomic DNA of A1501 and cloned into pLAFR3. The resulting complementing plasmid was then introduced into the WT or mutant strain by triparental mating, generating complemented strains (Table S3). The gene expression levels in the overexpression strains were confirmed to be higher than those in the WT strain using qRT-PCR.

The *ΔcrcZΔcrcY* double mutant was constructed using the *ΔcrcZ* mutant as the parental strain. Briefly, a fragment that contained the Cm resistance cassette located between the upstream and downstream DNA fragments of *crcY* was generated by overlap extension PCR using the strategy of PCR-based fusions.[89] The fusion PCR product was then cloned into the multiple cloning site of the pMD18-T vector (TaKaRa, Japan). The resulting plasmid DNA was double digested with *Xba* I/*Sph* I and then cloned into the same site of pK18mob*sacB*.[86] The resulting plasmid was introduced into the genome of *ΔcrcZ* by triparental mating and a double recombinant was selected based on sucrose resistance. Correct recombination in the resulting *ΔcrcZΔcrcY* mutant was checked by PCR using the primers M-*crcY2*(up)-F and M-*crcY2* (down)-R (Table S4), followed by nucleotide sequencing of the obtained PCR products. In the same way, we also constructed the Δ*hfq*Δ*crc* mutant using *Δhfq* as the starting strain. Similarly, a fragment containing the Spc resistance cassette located between the upstream and downstream DNA fragments of *crc* was cloned between the *Nhe* I and *Eco*R I sites of pK18mob*sacB,* generating the plasmid pK18*crc,* and then was introduced into the genome of *Δhfq*. Correct recombination in the resulting *ΔcrcZΔcrcY* double mutant was checked by PCR.

Construction of translational *lacZ* fusions and β-galactosidase assay

To construct translation gene fusions, the DNA fragments that carried the respective promoter of the target gene were amplified by using the primers *edd-lacZ* F/*edd-lacZ* R2 and *gltR-lacZ* F/*gltR-lacZ* R2 (Table S4) and cloned into plasmid pXY2, a modified version of pUC18-mini-Tn7-Gm-*lacZ*.[87] The recombinant plasmid of pXY2 was electroporated into *P. stutzeri* A1501 together with pUX-BF13, and the mini-Tn7 element carrying the *lacZ* reporter fusion was integrated into the unique Tn7 site located downstream of *glmS*.[85] Specific β-galactosidase activity from bacterial suspensions growing in liquid cultures was measured by using 4-methylumbelliferyl-b-D-galactoside (4MUG) as the enzymatic substrate. The fluorescent product, 7-hydroxy-4-methylcoumarin (4MU), was detected at 460 nm after excision at 365 nm using a FlexStation 3 Plate Reader (Molecular Devices). Enzyme activity was reported as μmol 4 MU min^{-1} mg^{-1} protein.

Biolog phenotype profiling

The 96-well Biolog GENIII MicroPlate (Catalogue No.1030) was used to measure the respiratory activity of A1501 on different carbon sources. Briefly, the cultures were incubated at 30°C until mid-logarithmic phase, after which cells were harvested and suspended in a special "gelling" inoculating fluid (IF) at the recommended cell density. A total of 100 μL of the bacterial suspension was used to inoculate each well of the GENIII MicroPlate. The microplates were placed in an OmniLog instrument (Biolog Inc.) programmed to run at 30°C for 48 h. During the incubation, increased respiratory activity is observed in the wells, and cells utilize a carbon source and generate oxidants that then oxidize tetrazolium redox dye, forming a purple colour. The formation of formazan was recorded at 15 min intervals, and data were analysed using OmniLog Kinetic and Parametric software (Biolog Inc.).

Rhizosphere colonization and competition assays

The 12-day-old seedlings were transferred to 150 mL tubes (four seedlings per tube) that contained 30 mL of minimal K medium supplemented with the indicated carbon sources, and then inoculated with the indicated strains to obtain a final concentration of approximately 10^8 total CFUs/mL. In competition experiments, strains were inoculated at a 1:1 ratio. To confirm starting ratios at a 1:1 ratio, colony counts were performed on the initial inoculum. After 24 h of incubation, seedlings were harvested and the leaves were cut off. Root tips were washed and resuspended in 10 mL phosphate-buffered saline (PBS: 137 mM NaCl, 2.7 mM KCl, 10 mM Na_2HPO_4, and 2 mM KH_2PO_4). Root-attached bacteria were recovered by vortexing roots for 1.0 min and plating the appropriate dilutions on LB agar plates supplemented with the appropriate antibiotics. The plates were incubated overnight at 30°C. The amount of cells per g of root was then determined by colony forming unit (CFU) counting. The results were normalized to the fresh weight of the root.

Strain competition experiment

Freshly cultivated *P. stutzeri* wild-type strain A1501 and mutants were combined at a 1:1 ratio, inoculated at a starting OD_{600} of 0.1 and grown for 24 h in LB. To confirm starting ratios at a 1:1 ratio, colony counts were performed on the initial inoculum. After 24 h of incubation, the cultures were serially diluted and plated on LB agar plates containing the relevant antibiotics to enable each strain to be counted.[90] The wild-type strain A1501 was used as the competitor in all experiments. The mutant fitness score ratio was calculated as the ratio of CFUs of each mutant to that of A1501.

Nitrogenase activity assays

The nitrogenase activity of bacteria in pure cultures was evaluated using the acetylene reduction assay.[58] Cells from an overnight culture in LB medium were centrifuged and resuspended in a 100 mL flask containing 10 mL of minimal medium K supplemented with the indicated carbon sources at an OD_{600} of 0.1. The suspension was incubated for 24 h at 30°C with vigorous shaking under an argon atmosphere containing 0.5% oxygen, and then 10% acetylene was added. Gas samples (0.25 mL) were taken at 2-h intervals to determine the amount of ethylene produced on a poly divinylbenzene porous bead GDX-502 column using an SP-2100 gas chromatograph fitted with a flame ionization detector (Beijing Beifen-Ruili Analytical Instrument Co. Ltd.). The ethylene content in the gas samples was determined by reference to an ethylene standard. The nitrogenase activity was expressed as nmol ethylene min^{-1} mg^{-1} protein. Protein concentrations were determined using the Bio-Rad protein assay reagent kit (Bradford, Bio-Rad).

Root-associated nitrogenase activity was measured using the acetylene reduction assay.[57] The 12-day-old seedlings were transplanted to 150 mL tubes (four seedlings per tube) that contained 30 mL of minimal K medium supplemented with the indicated carbon sources, and then inoculated with the indicated strains at a final OD_{600} of 0.1. The tubes sealed with rubber septa were injected with 10% (vol/vol) pure acetylene, and ethylene concentrations were measured at 2-h intervals for 24 h at 30°C under static conditions. Ethylene production from uninoculated seedlings in the presence of 10% acetylene and inoculated seedlings in the presence of air was also assayed to determine the background ethylene emission of rice as a plant hormone.

Total RNA isolation and quantitative real time RT-PCR (qRT-PCR) analysis

To determine the expression of the indicated genes in pure bacterial cultures, total RNA was isolated with an innuPREP RNA Mini Kit (Analytik Jena) according to the manufacturer's instructions. Total RNA was

reverse transcribed using random primers and the High Capacity cDNA Transcription Kit (Applied Biosystems) according to the manufacturer's instructions. PCR was carried out with Power SYBR Green PCR Master Mix on an ABI Prism 7500 Sequence Detection System (Applied Biosystems) according to the manufacturer's recommendations. The 16S rRNA gene was used as the endogenous reference control, and relative gene expression was determined using the comparative threshold cycle $2^{-\Delta\Delta CT}$ method. Data were analysed using ABI PRISM 7500 Sequence Detection System Software (Applied Biosystems). Primers were designed based on the full genome sequence of *P. stutzeri* A1501, and they are listed in Table S4.

Twelve-day-old seedlings were transferred to 150 mL tubes (four seedlings per tube) containing 30 mL of minimal K medium supplemented with the measured carbon sources, and then inoculated with the indicated strains at a final OD_{600} of 0.1 to determine the expression of genes in *P. stutzeri* A1501 associated with host rice roots. After 8 h of incubation, root tips were placed on 20 mL of 60% (v/v) RNAlater solution (Invitrogen) in PBS. Root-attached bacteria were removed from roots by vortexing for 1.0 min, harvested by quick centrifugation (18,900 × g, 1 min, 4°C), and re-suspended in cold lysis buffer (Analytik Jena). Total RNA was isolated with an innuPREP RNA Mini Kit (Analytik Jena), and qRT-PCR was performed using SYBR Premix Ex Taq (TaKaRa) and gene-specific primers (Table S4).

5′ rapid amplification of cDNA ends (5′ RACE) to determine transcriptional start sites

The transcriptional start of CrcZ and CrcY was determined using 5′ RACE (Invitrogen) according to the manufacturer's instructions. Briefly, first-strand cDNA was synthesized using the primer GSP1, which was specific for the target gene sequence. The purified cDNA was tailed with dCTP by terminal deoxynucleotidyl transferase. PCR amplification was performed using the sequence-specific primer GSP2 and the anchor primer AAP. The primers GSP1 and GSP2, which are specific for the target gene tested here, are listed in Table S3. The 5′ RACE products were cloned into the pGEM-T Easy vector (Promega) and sequenced to map the 5′ end of the transcript.

Absolute quantification of the RNA copy number using droplet digital PCR (ddPCR)

Quantification by ddPCR was performed in 20 μL reaction mixtures containing 10 μL of 2 × EvaGreen ddPCR SuperMix (Bio-Rad) and primers at a final concentration of 0.2 μM were included. No template controls were used to monitor contamination and primer-dimer formation. Reactions were equilibrated for 3 min at room temperature and dispensed into each well of the droplet generator DG8 cartridge (Bio-Rad). Each oil compartment of the cartridge was filled with 70 μL of droplet generation oil for EvaGreen (Bio-Rad), and approximately 20,000 droplets were generated in each well using the droplet generator (Bio-Rad, QX200). The entire droplet volume (40 μL) was subsequently loaded onto a 96-well PCR plate and then heat sealed with a pierceable foil in the PX1 PCR Plate Sealer (Bio-Rad). The optimal thermal cycling conditions were used as follows: 95°C for 5 min; 40 cycles of 95°C for 30 s, 58°C for 1 min; and then 98°C for 10 min. The cycled droplets were read individually with the QX 200 droplet reader (Bio-Rad) and analysed with QuantaSoft droplet reader software.

Microscale thermophoresis (MST) analysis

DNA templates that carried the wild or mutated *crcZ* (339 bp), *crcY* (315 bp), *oprB* (1254 bp), *gltR* (761 bp), *zwf* (1486 bp), *citN* (1344 bp), *benR* (984 bp), and *nifH* (882 bp) were synthesized by Sangon Biotech Co. All the synthesized DNA templates were sequenced to assure the absence of undesired mutations. For *in vitro* transcription from synthesized templates, the T7 High Yield RNA Transcription Kit (Vazyme) was used according to the manufacturer's instructions. The resulting ssRNA oligonucleotides were purified by the RNAClean XP (Beckman Coulter Inc.) according to the manufacturer's instructions. The purified Crc and Hfq proteins were labelled with a Monolith NT^{TM} Protein labelling kit RED-NHS according to the manufacturer's instructions (No. MO-L011, NanoTemper Technologies). For the measurements, the concentration of the labelled Hfq (20 nM) or Crc (200 nM) proteins was kept constant, while the concentrations of non-labelled ssRNA oligonucleotides varied from 0.3 μM to 10 μM. The dissociation constants (K_d) were calculated.[91] Data analyses were performed with NanoTemper Analysis software (NanoTemper Technologies).

Expression and purification of Hfq for MST measurements

The Hfq protein was expressed and purified using the Strep-Tactin system (IBA Life Sciences). To this end, a 255 bp DNA fragment containing the entire *hfq* ORF except the stop codon was amplified by PCR using the

oligonucleotides str-*hfq* F/str-*hfq* R (Table S4). The resulting product was double-digested with *Nde* I/*Xho* I and then ligated into the corresponding sites of plasmid pET30a, generating the plasmid pET31a-Hfq. The *E. coli Δhfq* strain (kindly provided by Yong Tao, the Institute of Microbiology of the Chinese Academy of Sciences, Beijing) containing the plasmid pET31a-Hfq was incubated in LB medium containing the appropriate antibiotic at 37°C with shaking to reach an OD_{600} of 0.6. At this point, expression of the Hfq protein was induced by adding isopropyl β-D-1-thiogalactopyranoside (IPTG) to a final concentration of 0.5 mM. After 6 h of incubation at 30°C, cells were harvested by centrifugation and resuspended in buffer W (100 mM Tris-HCl, pH 8.0, 150 mM NaCl, 1 mM EDTA). The cells were disrupted by sonication after eliminating cell debris by centrifugation (10,000 rpm, 4°C) for 30 min, and the supernatant was loaded onto a Strep-Tactin column (IBA Life Sciences). The column was extensively washed with wash buffer (250 mM NaCl, 50 mM Tris-HCl, pH 7.5). The Hfq protein was eluted with wash buffer (100 mM Tris-HCl, 150 mM NaCl, pH 8.0, 1 mM EDTA, and 50 mM biotin) and analysed using SDS-PAGE. The protein concentration was determined using the Bio-Rad protein assay reagent kit (Quick Start Bradford, Bio-Rad). Final preparations were stored at −80°C in storage buffer (20 mM Tris-HCl, pH 8.0, 200 mM NaCl, and 30% glycerol) until use.

Expression and purification of Crc and CbrB

The Crc protein was expressed and purified using the IMPACT™ (Intein Mediated Purification with an Affinity Chitin-binding Tag) system according to the manufacturer's instructions (New England Biolabs). A 777 bp fragment, which covers the entire coding region of the *crc* gene but excludes the termination codon, was amplified by PCR using pTW *crc* F/pTW *crc* R (Table S4). The resulting fragment was cloned between the *Nde* I and *Xho* I sites of the P_{T7} expression vector pTWIN1, generating the plasmid pTWIN1-Crc, which carries an in frame fusion at the 3′-end of the *crc* gene with codons for the intein/chitin-binding domain to allow purification through a chitin column. The *E. coli Δhfq* strains containing the plasmid pTWIN1-Crc were incubated in LB medium containing the appropriate antibiotic at 37°C with shaking to reach an OD_{600} of 0.6. At this point, expression of the Crc protein was induced by the addition of IPTG to a final concentration of 0.5 mM. After 6 h of incubation at 30°C, the cells were harvested by centrifugation and resuspended in elution buffer (20 mM HEPES, 500 mM NaCl, 0.1 mM EDTA, pH 8.0). The cells were disrupted by sonication, cell debris was eliminated by centrifugation (10,000 rpm, 4°C) for 30 min, and the supernatant was loaded onto a chitin column. The column was extensively washed with wash buffer (20 mM HEPES, pH 8.0, 500 mM NaCl, and 0.1 mM EDTA). The Crc-intein fusion was cleaved by an overnight treatment at 4°C with elution buffer containing 30 mM dithiothreitol (DTT). The untagged Crc protein was eluted from the column, dialyzed against a buffer (500 mM NaCl and 20 mM HEPES, pH 8.0), and concentrated using 3K Amicon filtration units. The purity of the protein was as high as 90%, as judged using SDS-PAGE. The protein concentration was determined using the Bio-Rad protein assay reagent kit (Quick Start Bradford, Bio-Rad). Final preparations were stored at −80°C in storage buffer (20 mM Tris-HCl, pH 8.0, 200 mM NaCl, and 30% glycerol) until subsequent MST measurements.

The CbrB protein was expressed and purified using the IMPACT™ system for DNase I footprinting assays.

Expression and purification of RpoN for DNase I footprinting assays

The pET-28a expression system (Novagen) was used to produce C-terminally His-tagged RpoN within host *E. coli* BL21 (DE3) cells. A fragment of *rpoN* was amplified by PCR using the pET28a-*rpoN*-F/R primers (Table S4). The PCR product was digested with *Nde* I and *Hind* III and ligated into the protein expression vector pET28a, which had been digested with the same enzymes. The resulting plasmid (pET28a-RpoN) was introduced into the *E. coli* BL21 strain. An overnight culture of BL21 harbouring the expression plasmid was used to inoculate LB medium containing the appropriate antibiotics. This cell culture was incubated with shaking at 37°C until the OD_{600} was 0.6 ∼ 0.9, at which point production of His-tagged RpoN was induced by the addition of IPTG to a final concentration of 0.1 mM. His-tagged RpoN was purified using a Ni-NTA Fast Start Kit (Qiagen, Venlo, Netherlands) according to the manufacturer's instructions. The purity of the protein was as high as 90%, as judged by SDS-Tris-glycine PAGE. His-tagged RpoN was quantitated using the Bio-Rad protein assay reagent kit (Quick Start™ Bradford, Bio-Rad) and stored at −80°C until further DNase I footprinting assays.

DNase I footprinting assays

DNase I footprinting assays were performed according to the manufacturer's instructions (Tolo Biotech).[92] The DNA probe was prepared by PCR amplification of the 264 bp CrcZ and 300 bp CrcY promoter regions

using the primers FP *crcZ* F/FP *crcZ* R and FP *crcY* F/FP *crcY* R (Table S4), respectively. For each assay, 300 ng probes were incubated with 5 μg purified RpoN and 15 μg purified protein CbrB in a total volume of 40 μL. After an incubation for 30 min at 30°C, 10 μL of a solution containing ~0.015 units of DNase I (Promega) and 100 nmol of freshly prepared $CaCl_2$ were added and a subsequent incubation was performed at 37°C for 1 min. The reaction was stopped by adding 140 μL DNase I stop solution (200 mM unbuffered sodium acetate, 30 mM EDTA, and 0.15% SDS). Samples were first extracted with phenol/chloroform and then precipitated with ethanol. Pellets were dissolved in 30 μL of MilliQ water. The preparation of the DNA ladder, electrophoresis, and data analysis were performed according to the manufacturer's instructions,[92] except that the GeneScan-LIZ600 size standard (Applied Biosystems) was used.

Determination of *nifH* mRNA stability

The stability of the *nifH* mRNA was determined in A1501 and the Δ*hfq* or Δ*hfq* (p*Lhfq*) strains grown under nitrogen fixation conditions for 6 h followed by the addition of rifampicin (400 μg/mL, final concentration). Aliquots were added to two volumes of RNA protect (Sigma). After incubating at room temperature for 5 min, the samples were centrifuged for 5 min at 4°C and 12,000 rpm, and the pellets were quickly frozen in liquid nitrogen and stored at −80°C until they were ready for use. Total RNA was isolated with an innuPREP RNA Mini Kit (Analytik Jena) according to the manufacturer's instructions. Full-length cDNAs were synthesized from total RNA using a First Strand cDNA synthesis kit (Takara Bio) and were used to estimate mRNA levels with qRT-PCR. The primers used to measure the mRNA half-life are listed in Table S4 (RT *nifH* F/RT *nifH* R). The relative mRNA concentration was calculated by the comparative threshold cycle ($2^{-\Delta\Delta CT}$) method with 16S rRNA as the endogenous reference. Data are presented as the percentage of *nifH* transcript levels relative to the amount of these transcripts at time point zero.

Exopolysaccharide isolation and quantification

The strains were grown in minimal medium K supplemented with 6 mM ammonium and different carbon sources at 30°C for 24 h. Then, the cultures were treated with 10% trichloroacetic acid (1:1), homogenized for 30 min, and centrifuged at 10,000 rpm for 30 min. Exopolysaccharides were isolated from culture supernatants by adding two volumes of chilled absolute ethanol. After further precipitation by cold absolute ethanol and lyophilization, purified exopolysaccharides were obtained.[93] The exopolysaccharides were quantified using the phenol-sulfuric acid method[94] and subsequently normalized to the total cellular protein level remaining after extraction, as determined using the Bio-Rad protein assay reagent kit (Quick Start™ Bradford, Bio-Rad). Final concentrations were expressed as mg exopolysaccharide per g bacterial protein.

HPLC analysis of glucose consumption

Culture samples (1.0 mL) were obtained at different time points on the growth curve and were centrifuged at 10,000 rpm for 30 min. The supernatant was collected and frozen at −80°C until HPLC analysis. The HPLC-RID system (Waters Corp.) equipped with a refractive index (RI) detector was used for each sample.[95] The injection volume was 10 μL and the mobile phase was a 50-mg/L EDTA-Ca water solution delivered at a flow rate of 0.5 mL/min. The column temperature was set at 90°C. The chromatography running time was 15 min. The HPLC peaks were identified to be glucose by comparing the retention time between them and the standard compound.

QUANTIFICATION AND STATISTICAL ANALYSIS

Unless stated otherwise, experiments were performed three times with similar results. Each bar on graphs represents a mean of biological replicates and error bars indicate the SEM (standard error of the mean), as mentioned in figure legends for each experiment. For all assays, n represents the number of biological replicates. Statistical analysis was performed using GraphPad Prism 9.0. A two-tailed unpaired Student's t-test with a 95% confidence interval was used to evaluate the difference between two groups. For more than two groups, one-way ANOVA was used. A probability value of $p \leq 0.05$ was considered significant. Data are presented as averages ± SEM. ****: $p \leq 0.0001$; ***: $p \leq 0.001$; **: $p \leq 0.01$; *: $p \leq 0.05$; and ns: non-significant.